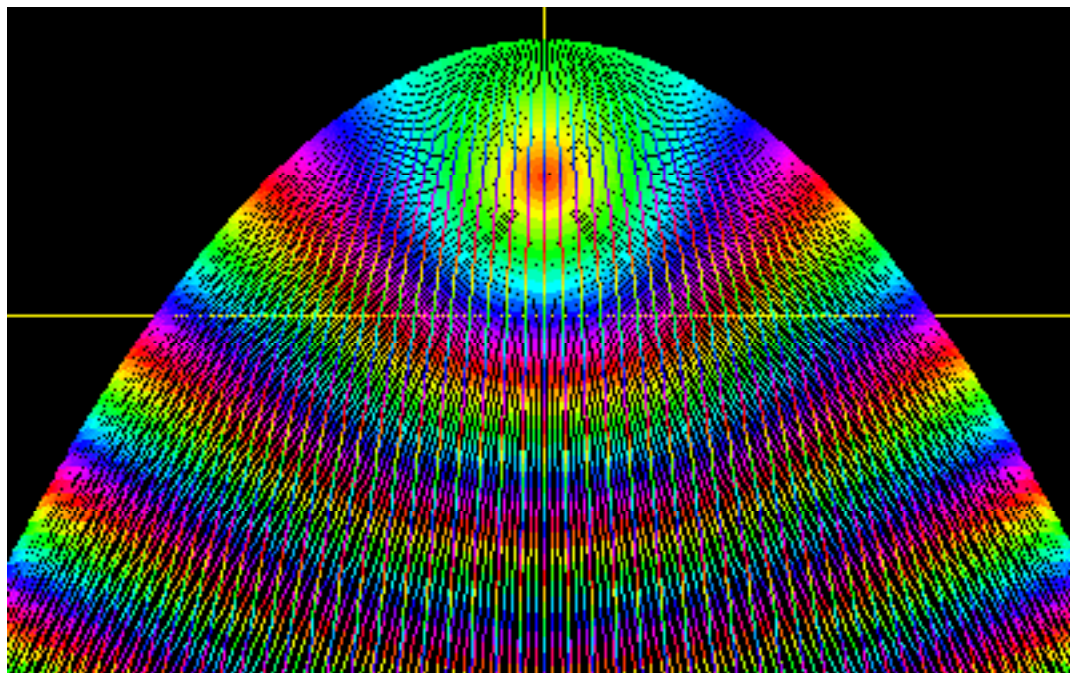


Unit 7

Action and Functional Variation



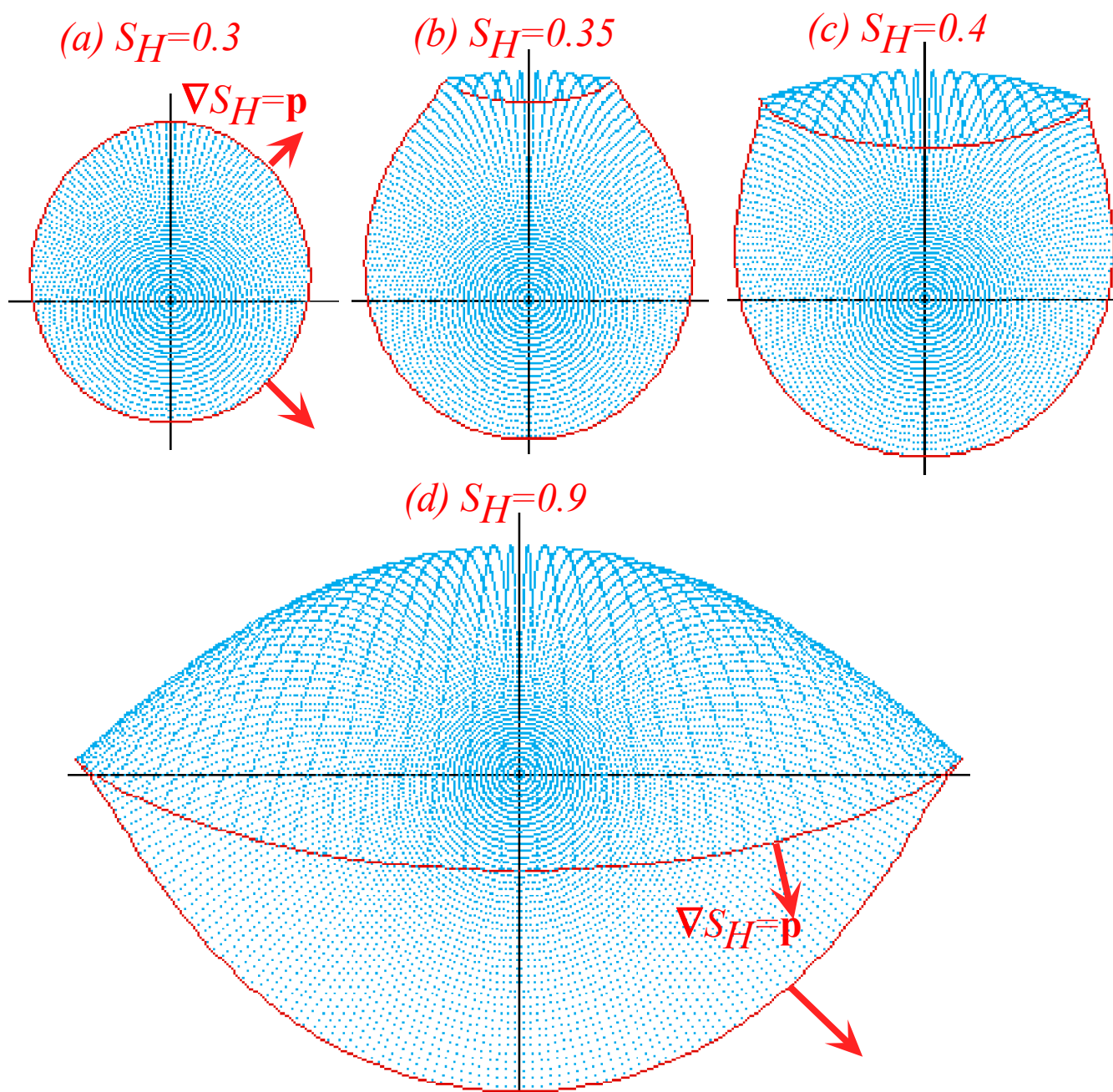
William G. Harter

Who or what makes the classical laws? Here we begin to see some of the deeper principles that underlie the classical façade of our world. Something called action seems to be in control and prefers lowest bidders.

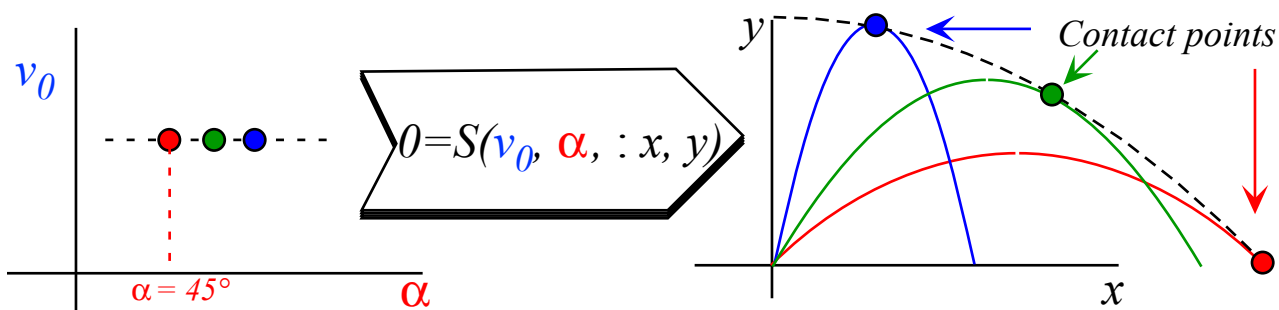
The minimization of entire families of functions is called calculus of variation or functional variation. It is introduced here in connection with the famous Hamilton's Principle function $S_p = \int L dt$ or action and Hamilton's Characteristic function $S_H = \int p dx$ or reduced action.

Why these two actions seek minimum or stationary values is a question that begs introduction of wave interference behavior in the form of the Hamilton-Jacobi equation. The HJ equation is an approximation to quantum wave theory that was discovered before the latter.

This old theory is still useful in the form of semi-classical mechanics that provides powerful approximate solutions to otherwise intractable quantum problems. Old ideas never die. They just lie in waiting.



Time evolution by contact transformation



UNIT 7 ACTION AND FUNCTIONAL VARIATION4

Chapter 7.1 Introduction4

Chapter 7.2 Variational Calculus5

 Solution 1. Solve Euler-Lagrange for $y(x)$ 6

 Solution 2. Use "pseudo-hamiltonian" conservation6

 Solution 3. Make y independent variable and use "pseudo-momentum" conservation7

 Solution 4. Obtain differential equations directly8

Chapter 7.3 Hamilton's Principle.....11

 (a) Geodesic curves13

 (b) Tautochrone-brachistichone curves15

 (c) Huygen's pendulum17

Chapter 7.4 Curve Families and Contact Relations19

 (a) Contact transformations21

 (b) Legendre transformations.....21

Chapter 7.5 Action: Generators of Active Contact Transformations25

 (a) Hamilton's characteristic action25

 (c) Example of H-J equations: Elementary trajectories27

 (d) Example of H-J wavefronts: wave and particle velocity30

Chapter 7.6 Time of Flight, Energy, and Action35

 (a) Quantum wave fronts vs. classical35

 (b) Huygen's principle: "Proof" of classical axioms36

Chapter 7.7 Action-Angle Variables : Semi-classical quantization39

 (a) 1-Dimensional vibration and rotation.....39

 (b) Multi-dimensional action angle analysis42

 (c) Action-color and Davis-Heller quantization.....43

 (d) A "clockwork universe"45

 (e) Non-linear modes: Action Fourier analysis.....46

Unit 7 Action and Functional Variation

Chapter 7.1 Introduction

POOF!Foop! Waves disappear then reappear elsewhere. They are *non-local* unlike our very local classical mechanics that decides at each point in space and time exactly how fast and where each mass or particle-coordinate should proceed in the next instant of time. This leads along a particular trajectory $q^k(t)$ or phase-space path $\{q^k(t), p_m(t)\}$ that is one of the solutions to a Newton, Lagrange, Riemann, or Hamilton set of differential equations treated in Units 1 thru 6.

Now we take a more global view of mechanical motion and ask what integral or global properties are peculiar to the trajectories or paths that massive bodies follow when they are obeying our various differential equations of motion. We will inquire about arbitrary kinds of *variation* from the "straight-and narrow" trajectory paths found so far, and thereby develop a type of mathematics which is known as the *calculus of variation*.

Variational calculus leads to path-integral equations as well as differential equations. A type of integrals known as *action integrals* will be discussed, in particular, *Hamilton's principle action* S_p which is the time integral of the Lagrangian

$$S_p = \int L dt \quad (7.1.1)$$

and *Hamilton's characteristic action* S_H which is the sum of areas swept out in phase space.

$$S_H = \int p_\mu dq^\mu \quad (7.1.2)$$

From Poincare's invariant equation (1.13.5) it follows that the two actions are closely related.

$$S_p = \int L dt = \int p_\mu dq^\mu - \int H dt = S_H - E \cdot t \quad (7.1.3)$$

The principle action is called that because it arises in the consideration of Hamilton's *least action principle* which will be one of the first things considered in this Unit.

The naming of the characteristic action is more obscure but no less interesting. The name comes from a method for solving wave equations which is called the *method of characteristics*. Using this method it is possible to obtain solutions to certain partial differential equations by ordinary integration along certain characteristic or "ray" curves. We shall see how families of particle trajectories are the characteristic rays of wave equations for Hamilton's characteristic function S_H . Such equations are known as *Hamilton-Jacobi* equations and perhaps the most esoteric form that Newton's original mechanical equations can take. However, they are the relations that forge connection to quantum wave mechanics and more basic statement of the laws of nature. Then, Newton's axioms are reduced to results of more basic axioms and seen to be only approximately true in the limit of high action.

In summary, this chapter is not so much concerned with single trajectories or functions; the techniques considered so far do that as well as we know how. Rather, this section is devoted to the study of whole *families* of trajectories or functions such as orbit clouds shown in Unit 5.

Chapter 7.2 Variational Calculus

Variational calculus is concerned with finding minimum or maximum values to integrals such as

$$I(y) = \int_{x_0}^{x_1} dx \lambda(y(x), y'(x), x) \tag{7.2.1}$$

where the curve $y(x)$ can vary at every point x . If $I(y)$ was a simple function like $I(y) = y^2 - 4y$ we would find zero (s) of its derivative $dI = (2y - 4)dy = 0$ at $y = 2$ and be done. However, here $I(y)$ is a *functional*, that is, a function $\int dx \lambda(y, y')$ of an entire function $y(x)$ and its derivative $y'(x)$ either of which can be varied arbitrarily at any point between x_0 and x_1 of the dependent integration variable as shown in Fig. 7.2.1. (It is possible that $\lambda(y, y', x)$ may have explicit x -dependence, as well.)

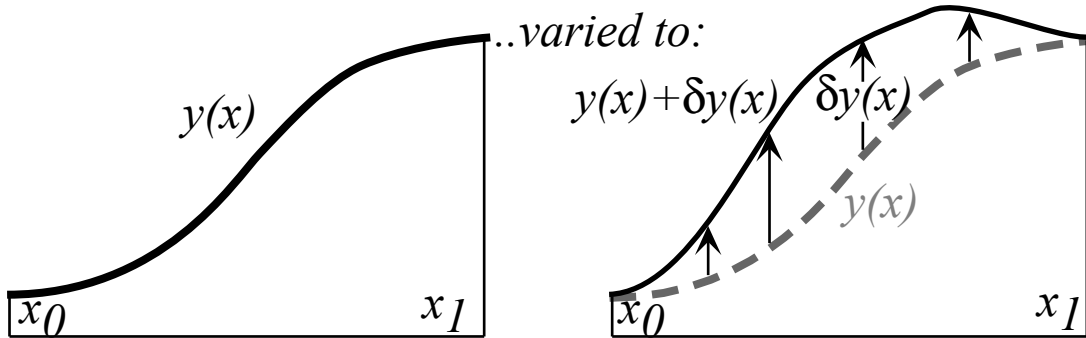


Fig. 7.2.1 Variation of function curve or path from $y(x)$ to $y(x) + \delta y(x)$.

As shown in the figure, an arbitrary but small variation function $\delta y(x)$ is allowed at every point x along the curve except at the end points x_0 and x_1 where, by definition

$$\delta y(x_0) = 0 = \delta y(x_1) \tag{7.2.2}$$

This changes integral (7.2.1) according to a Taylor series of first order.

$$I(y + \delta y) = \int_{x_0}^{x_1} dx \left[\lambda(y, y', x) + \frac{\partial \lambda}{\partial y} \delta y + \frac{\partial \lambda}{\partial y'} \delta y' \right] \quad \text{where: } \delta y' = \frac{d}{dx} \delta y \tag{7.2.3}$$

Replacing $\frac{\partial \lambda}{\partial y'} \delta y'$ with $\frac{d}{dx} \left(\frac{\partial \lambda}{\partial y'} \delta y \right) - \frac{d}{dx} \left(\frac{\partial \lambda}{\partial y'} \right) \delta y$ gives

$$\begin{aligned} I(y + \delta y) &= \int_{x_0}^{x_1} dx \left[\lambda(y, y', x) + \frac{\partial \lambda}{\partial y} \delta y - \frac{d}{dx} \left(\frac{\partial \lambda}{\partial y'} \right) \delta y \right] + \int_{x_0}^{x_1} dx \frac{d}{dx} \left(\frac{\partial \lambda}{\partial y'} \delta y \right) \\ &= \int_{x_0}^{x_1} dx \lambda(y, y', x) + \int_{x_0}^{x_1} dx \left[\frac{\partial \lambda}{\partial y} - \frac{d}{dx} \left(\frac{\partial \lambda}{\partial y'} \right) \right] \delta y + \left(\frac{\partial \lambda}{\partial y'} \delta y \right) \Bigg|_{x_0}^{x_1} \end{aligned} \tag{7.2.4}$$

The third and last term vanishes by (7.2.2) leaving a total first order variation δI as follows.

$$\delta I = I(y + \delta y) - I(y) = \int_{x_0}^{x_1} dx \left[\frac{\partial \lambda}{\partial y} - \frac{d}{dx} \left(\frac{\partial \lambda}{\partial y'} \right) \right] \delta y \tag{7.2.5a}$$

If integral I is a minimum or maximum its first order variation δI must be zero for all $\delta y(x)$ even if it is only non-zero for a small region of the x interval. So, the I integrand must be zero everywhere.

$$\delta I = 0 \Rightarrow \frac{d}{dx} \left(\frac{\partial \lambda}{\partial y'} \right) - \frac{\partial \lambda}{\partial y} = 0 \tag{7.2.5b}$$

The result is called an *Euler-Lagrange equation*. It has the form of a 1-D Lagrange equation

$$\frac{d}{dt} \left(\frac{\partial L}{\partial \dot{q}} \right) - \frac{\partial L}{\partial q} = 0 \tag{7.2.5c}$$

with λ , y , y' , and x replaced with L , q , \dot{q} , and t , respectively. Indeed, it will be shown that Lagrange's equations guarantee that the principle action integral S_p of (7.1) always accumulates a minimum value along any trajectory and hence must do so consistently along each infinitesimal segment of any path.

As in trajectory problems, the writing of Lagrange equations is one task, but finding useful solutions may be quite another. For example, let a string of beads of density ρ hang on a curve $y=y(x)$ so the integral V over gravitational potential $\rho g y(x) ds$ of each line segment ds is minimum.

$$V = \int \rho g y ds = \rho g \int y \sqrt{dx^2 + dy^2} = \rho g \int dx y \sqrt{1 + y'^2} \tag{7.2.6}$$

Several methods for finding the desired minimizing curve $y=y(x)$ need to be exposed and compared.

Solution 1. Solve Euler-Lagrange for y(x)

The pseudo-lagrangian integrand function in (7.2.6) is $\lambda(y, y') = y \sqrt{1 + y'^2}$. Its Euler-Lagrange equation has fairly complicated parts.

$$\frac{\partial \lambda}{\partial y} = (1 + y'^2)^{1/2}, \quad \frac{\partial \lambda}{\partial y'} = (1 + y'^2)^{-1/2} y y', \quad \frac{d}{dx} \frac{\partial \lambda}{\partial y'} = \frac{y'' y + y'^2 + y'^4}{(1 + y'^2)^{1/2}} \tag{7.2.7}$$

The solution of the resulting equation is not immediately obvious so it is left as an exercise!

$$y'' y = 1 + y'^2 \tag{7.2.8}$$

Solution 2. Use "pseudo-hamiltonian" conservation

The pseudo-lagrangian integrand function $\lambda(y, y') = y \sqrt{1 + y'^2}$ is independent of x . This is just like a Lagrangian $L(q, \dot{q})$ with no time dependence which allows a constant Hamiltonian $H = p \dot{q} - L$. Here x independence implies a constant or conserved pseudo-hamiltonian h defined as follows.

$$const. = h = p y' - \lambda = y' \frac{\partial \lambda}{\partial y'} - \lambda = (1 + y'^2)^{-1/2} y y' - (1 + y'^2)^{1/2} y$$

This simplifies easily to a common integral.

$$h^2 = \frac{y^2}{1 + y'^2}, \quad h y' = \sqrt{y^2 - h^2}, \quad \int dx = \int \frac{h dy}{\sqrt{y^2 - h^2}} = h \cosh^{-1} y \tag{7.2.9}$$

The result is a beautiful hyperbolic catenary curve of the St. Louis arch by Eero Saarinen. (Fig. 7.2.2)

$$y(x) = h \cosh (x/h) \tag{7.2.10}$$

A hanging catenary chain (Fig. 7.2.3) has all tension forces lined up with the tangent at every point, and so must the inverted catenary of St. Louis have all compressive loads centered on tangents, as well. One might imagine a thousand hanging chains all welded into a solid so it would stand upside down without buckling. All its arch curves, inside and out, belong to a family of congruent hyperbolic cosines.

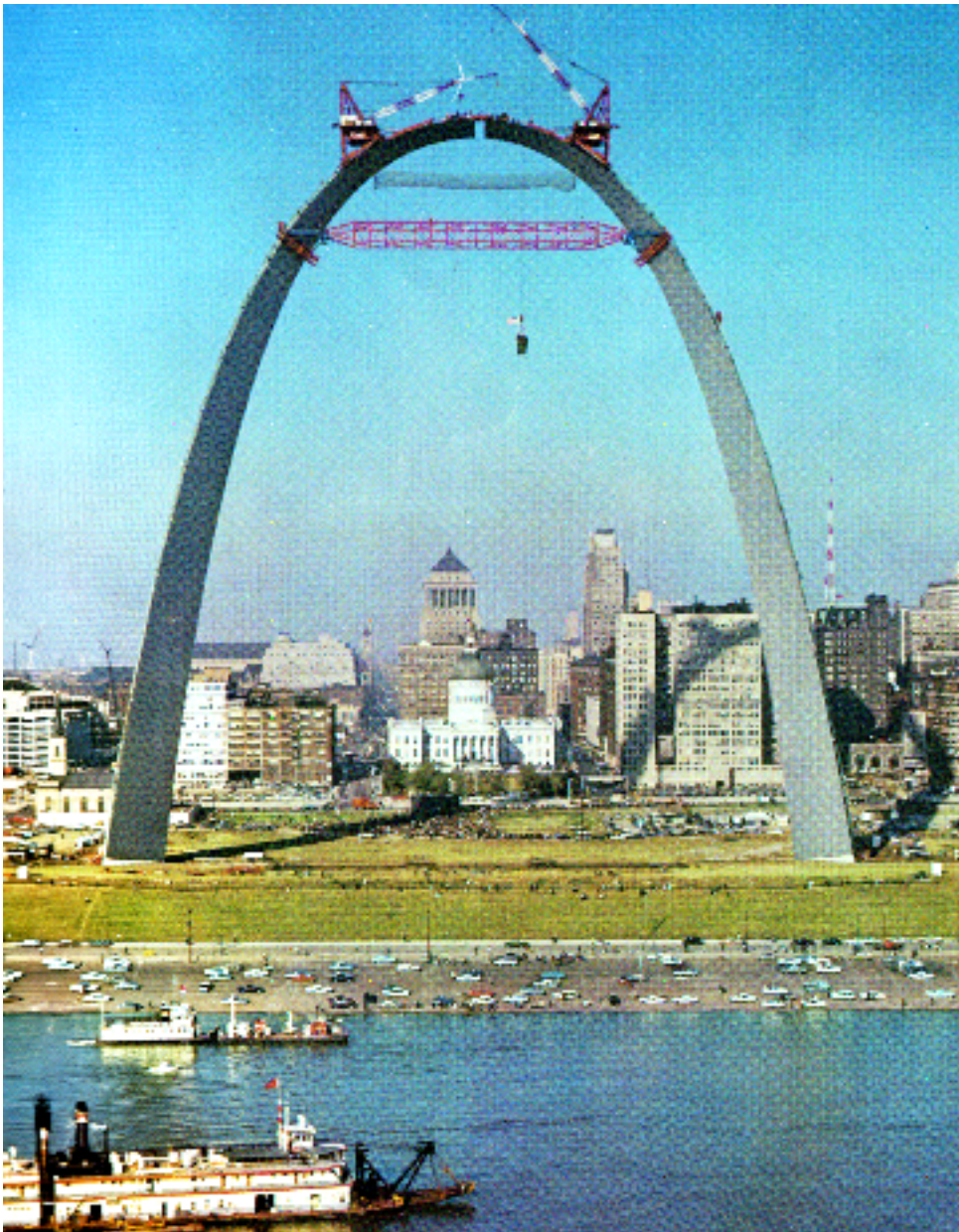


Fig 7.2.2 St. Louis Arch (Jefferson National Monument) is being "topped-out" as the final segment is lifted into place on October 28 1965. A 450-ton force is being applied to separate the arms for the final segment that will match its gap to within a fraction of a millimeter and allow closure.

Solution 3. Make y independent variable and use "pseudo-momentum" conservation

Converting the integral (7.2.6) over x to a y -integral gives a different pseudo-lagrangian Λ as follows.

$$\begin{aligned} V &= \rho g \int dx y \sqrt{1+y'^2} = \rho g \int dy \frac{dx}{dy} y \sqrt{1+y'^2} \\ &= \rho g \int dy \Lambda(x, x'), \quad \text{where: } \Lambda(x, x') = y \sqrt{x'^2 + 1} \end{aligned}$$

Pseudo-lagrangian Λ has no x -dependence which implies a constant pseudo-momentum p , as follows.

$$\frac{\partial \Lambda(x, x')}{\partial x} = 0 \text{ implies: } \text{const.} = p = \frac{\partial \Lambda(x, x')}{\partial x'} = \frac{yx'}{\sqrt{x'^2 + 1}} \tag{7.2.11}$$

There immediately results a hyperbolic cosine like that of (7.2.10) and Fig. 7.2.2..

$$dx = \frac{pdy}{\sqrt{y^2 - p^2}}, \quad y = p \cosh \frac{x}{p} \tag{7.2.12}$$

Solution 4. Obtain differential equations directly

The most elegant solutions might not be the best for all occasions! Consider the differential analysis of tension vectors from one link of a chain to the next as sketched in Fig. 7.2.3. At the same time we can compare a catenary arch (Fig. 7.2.4a) with an arch of a suspension bridge. (Fig. 7.2.4b)

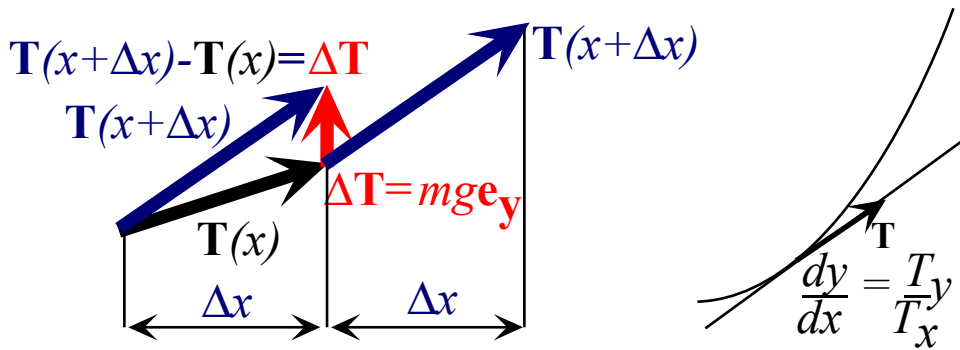


Fig. 7.2.3 Variation of tension vector from $\mathbf{T}(x)$ to $\mathbf{T}(x+dx)$.

(a) Catenary Arch

(b) Suspension Arch

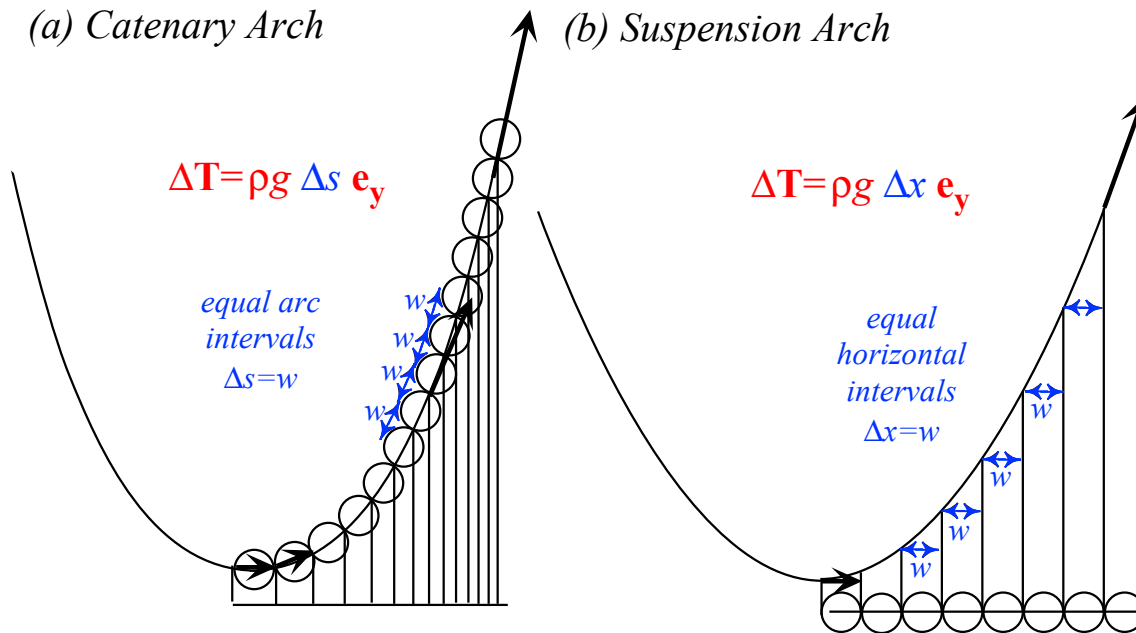


Fig. 7.2.4 Comparison of supporting arch curves. (a) Catenary, (b) Suspension bridge

The first differential relation, shown on the right of Fig. 7.2.3, simply demands tension tangency.

$$\frac{dy}{dx} = y' = \frac{T_y}{T_x} \tag{7.2.13}$$

A second order differential equation relates arch curvature to the extra weight $\Delta T=mg$ of each link or bead supported by the arch. As shown in Fig. 7.2.3, the extra weight increases y-component T_y by

$$\Delta T = T_y(x+\Delta x) - T_y(x) = mg$$

The preceding relations are used in the derivative.

$$\frac{d^2y}{dx^2} = y'' = \lim_{\Delta x \rightarrow 0} \frac{y'(x+\Delta x) - y'(x)}{\Delta x} \equiv \frac{1}{\Delta x} \left(\frac{T_y(x+\Delta x)}{T_x(x+\Delta x)} - \frac{T_y(x)}{T_x(x)} \right) \equiv \frac{\Delta T}{T_x \Delta x} \tag{7.2.13}$$

The x-component T_x of tension is constant. The y-equation depends on y-tension increment as shown in Fig. 7.2.4(a) for a catenary ($\Delta T = \rho g \Delta s$) or in Fig. 7.2.4(b) for the suspension arch ($\Delta T = \rho g \Delta x$).

$$y'' = \frac{1}{T_x} \frac{dT}{dx} = \frac{\rho g}{T_x} \frac{ds}{dx} \quad \text{For: } \Delta T = \rho g \Delta s \qquad y'' = \frac{1}{T_x} \frac{dT}{dx} = \frac{\rho g}{T_x} \quad \text{For: } \Delta T = \rho g \Delta x$$

$$= \frac{\rho g}{T_x} \sqrt{1 + \left(\frac{dy}{dx}\right)^2} = \frac{\rho g}{T_x} \sqrt{1 + y'^2}$$

The catenary arch is hyperbolic.(Fig. 7.2.4(a)) The suspension arch is a parabola.(Fig. 7.2.4(b))

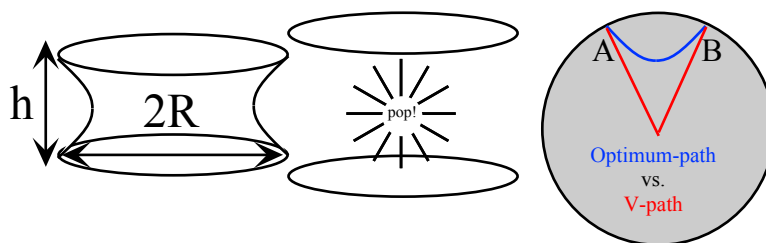
$$y' = \sinh \frac{\rho g(x+a)}{T_x} \tag{7.2.14a}$$

$$y = \frac{T_x}{\rho g} \cosh \frac{\rho g(x+a)}{T_x} + b$$

$$y' = \frac{\rho g}{T_x} x + a \tag{7.2.14b}$$

$$y = \frac{\rho g}{2T_x} x^2 + ax + b$$

This shows a subtle difference between the St. Louis arch (Jefferson monument) and more common arches of San Francisco (Golden Gate), New York (Brooklyn, George Washington, Veranzo, etc.).



Exercise 7.2.1 Extreme soap films

A soap film is stuck outside a pair of pair of circular rings separated by height h as shown above. What curve do you get if the film is stable? As h increases when does the film “pop” as sketched.

Exercise 7.2.2 Earth tunnels revisited

What curved tunnel inside the Earth minimizes travel time in the manner of Exercise 1.9.3 for Unit 1? As in the previous exercise involving V-shaped tunnels, assume a uniform density Earth.

Exercise 7.2.3 Tornado alley

What is the curve of a tornado funnel or a bathtub drain vortex?

Solve the problem assuming a *curl-free flow* that conserves angular momentum as in the $f(z)=Ai/z$ complex flow field shown in Fig. 1.10.10b in Ch. 10 of Unit 1. (Also, show the flow when A is complex, for example $A=I+i$.)[†]

First solve an easier problem for *constant-curl flow*, that is, rigid rotation. This is usually more appropriate at the bottom region of a bathtub vortex. (The two together are quite analogous to Fig. 1.9.7 showing Earth PE inside and out. Discuss.)

[†]Don't neglect Solution 4.

Chapter 7.3 Hamilton's Principle

We now consider Hamilton's principle time integral S_p of a generalized coordinate Lagrangian.

$$S_p(q) = \int_{t_0}^{t_1} dt L(q^\mu(t), \dot{q}^\mu(t), t) \quad (7.3.1)$$

As shown in Fig. 7.3.1 each trajectory curve $q^1(t)=x(t)$ or $q^2(t)=y(t)$ may vary everywhere except at end points t_0 and t_1 where, a definition similar to that used in (7.2.2) "pinches" the beginning and end.

$$\delta q^\mu(t_0) = 0 = \delta q^\mu(t_1) . \quad (7.3.2)$$

This changes integral (7.3.1) according to a Taylor series of first order.

$$S_p^{(1)}(q + \delta q) = \int_{t_0}^{t_1} dt \left[L(q(t), \dot{q}(t), t) + \frac{\partial L}{\partial q^\mu} \delta q^\mu + \frac{\partial L}{\partial \dot{q}^\nu} \delta \dot{q}^\nu \right] \quad \text{where: } \delta \dot{q}^\mu = \frac{d}{dt} \delta q^\mu \quad (7.3.3)$$

Replacing $\frac{\partial L}{\partial \dot{q}^\nu} \delta \dot{q}^\nu$ with $\frac{d}{dt} \left(\frac{\partial L}{\partial \dot{q}^\nu} \delta q^\nu \right) - \frac{d}{dt} \left(\frac{\partial L}{\partial \dot{q}^\nu} \right) \delta q^\nu$ gives an integration by parts.

$$\begin{aligned} S_p^{(1)}(q + \delta q) &= \int_{t_0}^{t_1} dt \left[L(q(t), \dot{q}(t), t) + \frac{\partial L}{\partial q^\mu} \delta q^\mu - \frac{d}{dt} \left(\frac{\partial L}{\partial \dot{q}^\nu} \right) \delta q^\nu \right] + \int_{t_0}^{t_1} dt \frac{d}{dt} \left(\frac{\partial L}{\partial \dot{q}^\nu} \delta q^\nu \right) \\ &= \int_{t_0}^{t_1} dt L(q(t), \dot{q}(t), t) + \int_{t_0}^{t_1} dt \left[\frac{\partial L}{\partial q^\mu} - \frac{d}{dt} \left(\frac{\partial L}{\partial \dot{q}^\mu} \right) \right] \delta q^\mu + \left(\frac{\partial L}{\partial \dot{q}^\nu} \delta q^\nu \right) \Big|_{t_0}^{t_1} \end{aligned} \quad (7.3.4)$$

The third and last term vanishes by (7.3.2) leaving a total first order variation δS_p as follows.

$$\delta S_p^{(1)} = S_p^{(1)}(q + \delta q) - S_p(q) = \int_{t_0}^{t_1} dt \left[\frac{\partial L}{\partial q^\mu} - \frac{d}{dt} \left(\frac{\partial L}{\partial \dot{q}^\mu} \right) \right] \delta q^\mu \quad (7.3.5a)$$

Suppose each coordinate $q^\mu(t)$ obeys Lagrange's equations, that is, (Recall (1.11.5) or (3.12.1d).)

$$\frac{\partial L}{\partial q^\mu} - \frac{d}{dt} \left(\frac{\partial L}{\partial \dot{q}^\mu} \right) = 0 \quad . \quad (7.3.5b)$$

This guarantees that $\delta S_p^{(1)} = 0$ so the action function S_p achieves an *extreme value* or *extremum* for $q^\mu(t)$. In other words, $q^\mu(t)$ could give for S_p a minimum value, a maximum value, or (most unpleasant) uncountable many inflection values. At this point we only know 1st-order variation is zero.

The second order variation involves only the following second order Taylor expansion terms if first-order variation (7.3.5a) vanishes with the Lagrange equations (7.3.5b).

$$\delta S_p^{(2)} = \int_{t_0}^{t_1} dt \frac{1}{2} \left[\frac{\partial^2 L}{\partial q^\mu \partial q^\nu} \delta q^\mu \delta q^\nu + 2 \frac{\partial^2 L}{\partial q^\mu \partial \dot{q}^\nu} \delta q^\mu \delta \dot{q}^\nu + \frac{\partial^2 L}{\partial \dot{q}^\mu \partial \dot{q}^\nu} \delta \dot{q}^\mu \delta \dot{q}^\nu \right] \quad (7.3.6a)$$

Let us consider the simplest example of this for one coordinate dimension and $L = L(q, \dot{q})$.

$$\delta S_p^{(2)} = \int_{t_0}^{t_1} dt \frac{1}{2} \left[\frac{\partial^2 L}{\partial q^2} (\delta q)^2 + 2 \frac{\partial^2 L}{\partial q \partial \dot{q}} \delta q \delta \dot{q} + \frac{\partial^2 L}{\partial \dot{q}^2} (\delta \dot{q})^2 \right] \quad (7.3.6b)$$

Lagrange equations (7.3.5b) equate $\frac{\partial L}{\partial q}$ with \dot{p} where $p = \frac{\partial L}{\partial \dot{q}}$ is the canonical momentum definition.

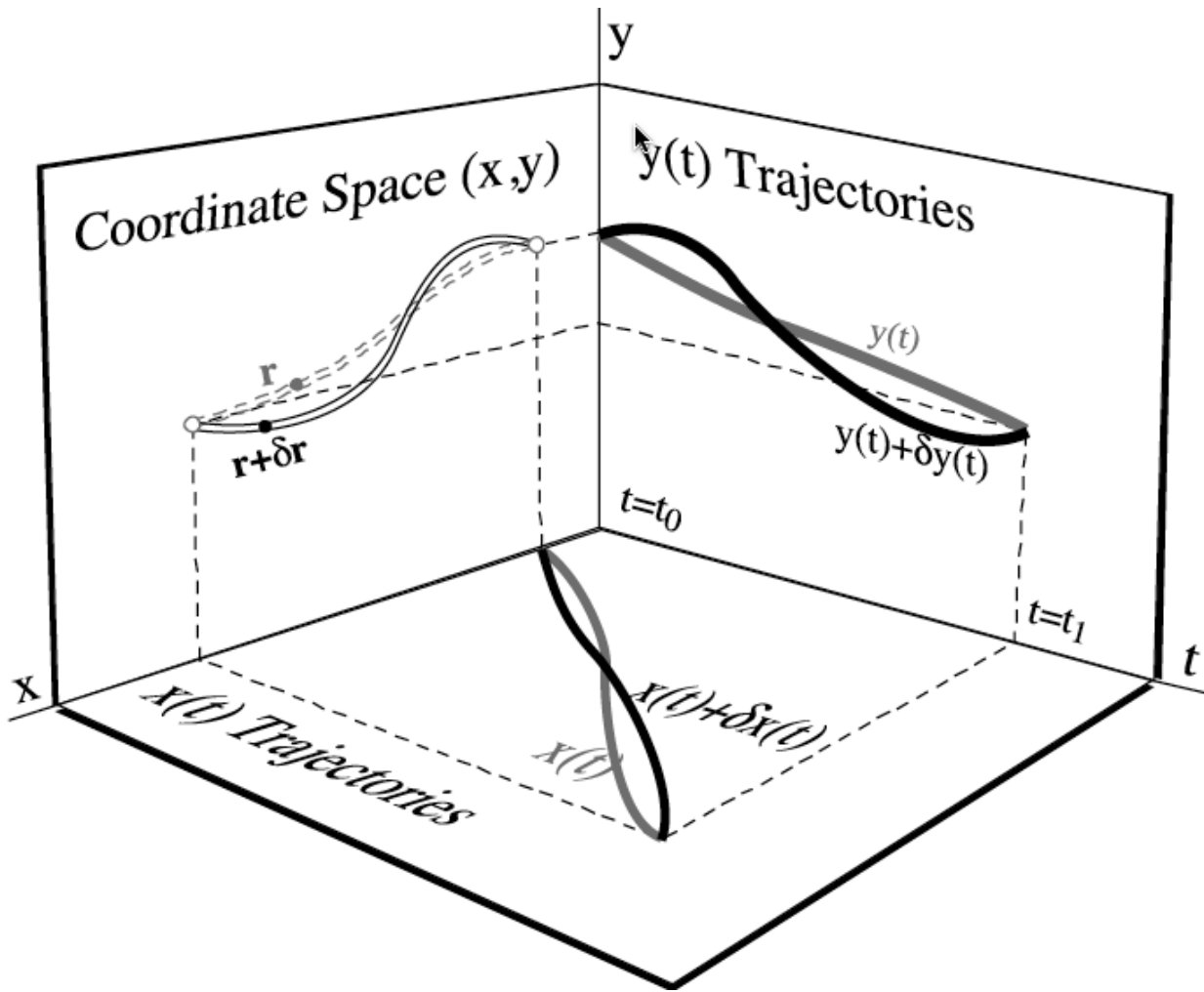


Fig. 7.3.1 Variation of paths and time trajectories for evaluating Hamilton's principle action S_p .

$$\delta S_p^{(2)} = \int_{t_0}^{t_1} dt \frac{1}{2} \left[\frac{\partial \dot{p}}{\partial q} (\delta q)^2 + 2 \frac{\partial p}{\partial q} \delta q \delta \dot{q} + \frac{\partial^2 L}{\partial \dot{q}^2} (\delta \dot{q})^2 \right] = \int_{t_0}^{t_1} dt \frac{1}{2} \left[\frac{\partial}{\partial q} \frac{d}{dt} [p(\delta q)^2] + \frac{\partial^2 L}{\partial \dot{q}^2} (\delta \dot{q})^2 \right] \quad (7.3.7)$$

If partial derivatives may be reordered, so may $\frac{d}{dt}$ and $\frac{\partial}{\partial q}$ in this case. (Recall *Lemma 2* (Eq. 1.5.2).)

$$\begin{aligned} \frac{\partial}{\partial q} \frac{df(q, \dot{q}, t)}{dt} &= \frac{\partial}{\partial q} \left[\dot{q} \frac{\partial f}{\partial q} + \ddot{q} \frac{\partial f}{\partial \dot{q}} + \frac{\partial f}{\partial t} \right] = \frac{\partial^2 f}{\partial q^2} \dot{q} + \frac{\partial^2 f}{\partial q \partial \dot{q}} \ddot{q} + \frac{\partial^2 f}{\partial q \partial t} \\ &= \left[\dot{q} \frac{\partial}{\partial q} + \ddot{q} \frac{\partial}{\partial \dot{q}} + \frac{\partial}{\partial t} \right] \frac{\partial f}{\partial q} = \frac{d}{dt} \frac{\partial f}{\partial q} \end{aligned} \quad (7.3.8)$$

Therefore the first term of (7.3.7) integrates out and vanishes at the end points according to (7.3.2). All that is left is inertia times velocity variation squared which is non-negative.

$$\delta S_p^{(2)} = \int_{t_0}^{t_1} dt \frac{1}{2} \frac{\partial^2 L}{\partial \dot{q}^2} (\delta \dot{q})^2 = \int_{t_0}^{t_1} dt \frac{I(q)}{2} (\delta \dot{q})^2 \geq 0 \quad (7.3.9)$$

The GCC second variation is the following and should be positive-definite, too. (See exercises)

$$\delta S_p^{(2)} = \int_{t_0}^{t_1} dt \frac{1}{2} \gamma_{\mu\nu} \delta \dot{q}^\mu \delta \dot{q}^\nu \geq 0 \quad (7.3.10)$$

If kinetic energy is positive, i.e., all eigenvalues of $\gamma_{\mu\nu}$ are positive definite, there follows *Hamilton's least action principle*; principle action S_p is *minimum* for classical paths no matter how negative may be the potential energy functions if they are continuous differentiable functions.

(a) Geodesic curves

If no potential is present ($V=0$) then the Lagrangian $L=T-V$ is reduced to its kinetic part alone.

$$L = T = \frac{1}{2} \gamma_{\mu\nu} \dot{q}^\mu \dot{q}^\nu = \frac{1}{2} m \left(\frac{ds}{dt} \right)^2 \quad (\text{for } : V = 0) \quad (7.3.11)$$

The GCC expression (3.7.4) or (3.9.10d) is given with the single-particle KE= $mv^2/2$. With no potential or explicit time dependence, a Lagrangian is also a Hamiltonian and is constant. (Recall (3.12.6).)

$$L = H = T = E = \text{const.} \quad (\text{for } : V=0) \quad (7.3.12)$$

This implies that the speed $v = \dot{s}$ is constant for a single particle on any coordinate manifold.

$$v = \frac{ds}{dt} = \dot{s} = \text{const.} \quad (\text{for } : V = 0) \quad (7.3.13)$$

The ($V=0$) principle action integral S_p can be written a number of ways for constant speed v .

$$S_p = \frac{1}{2} \int_{t_0}^{t_1} dt \gamma_{\mu\nu} \dot{q}^\mu \dot{q}^\nu = \frac{m}{2} \int_{t_0}^{t_1} dt \left(\frac{ds}{dt} \right)^2 = \frac{mv^2}{2} \int_{t_0}^{t_1} dt = \frac{mv}{2} \int_{s_0}^{s_1} ds \quad (7.3.10)$$

Hamilton's least-action principle demands minimum time $\int dt$ and minimum distance $\int ds$ for all paths on a GCC manifold if no potential or forces other than coordinate constraints are present. Curves of minimum time are called *tautochrones* and curves of minimum length are called *geodesics*.

The geodesic equations are simply the force-free Riemann's equation (3.10.10).

$$\ddot{q}^k + \Gamma_{m\ell}^k \dot{q}^m \dot{q}^\ell = 0 \quad (7.3.11a)$$

As discussed in Ch. 3, these are the Euler-Lagrange equations in GCC form. They correspond to zero intrinsic derivative equations for momentum $p^\mu = \dot{q}^\mu$ and p_μ according to (3.10.11a-b).

$$\frac{\delta p^k}{\delta t} = 0 = \dot{p}^k + \Gamma_{m\ell}^k p^m \dot{q}^\ell = \ddot{q}^k + \Gamma_{m\ell}^k \dot{q}^m \dot{q}^\ell \quad (7.3.11a)$$

$$\frac{\delta p_k}{\delta t} = 0 = \dot{p}_k - \Gamma_{kn}^m p_m \dot{q}^n \quad (7.3.11c)$$

Examples of surface geodesics are shown in Fig. 7.3.2 for a circular cone and paraboloid. The curvature of the surface causes a particle or a light ray to curve around the symmetry axis of these figures. Often, these are used as analogies for gravitational attraction in a curved space-time continuum. Fig. 7.3.2a has been used as a model for a "cosmic string" in which a dense line of matter or ant-matter distorts a flat-space vacuum. However, there are serious objections to such analogies some of which are brought up in the exercises. We imagine Fig. 7.3.2a as a model for an outer-space bowling alley having an automatic ball-return! (See Exercises 5.2.4 and 5.2.5 in Unit 5.)

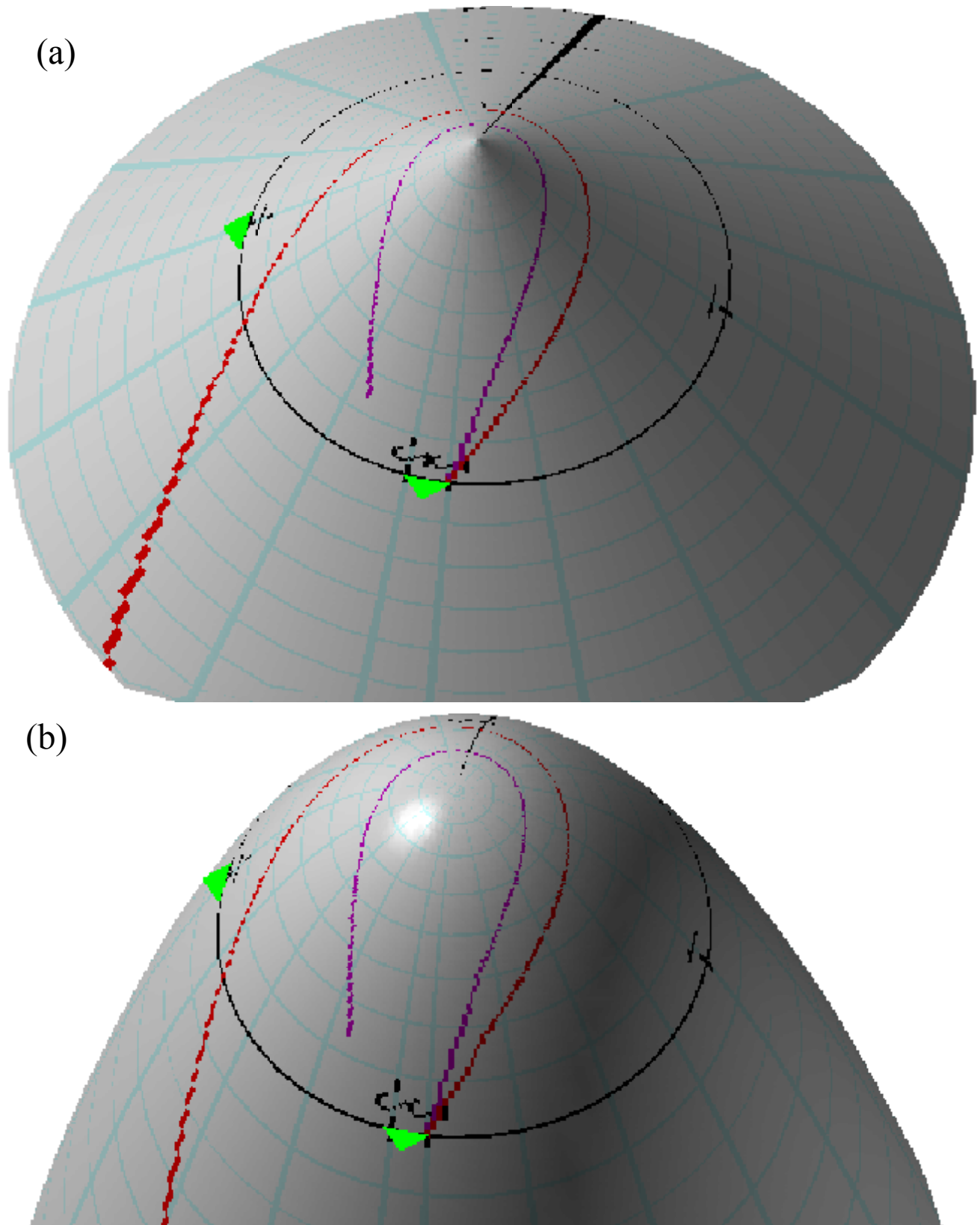


Fig. 7.3.1 Geodesic curves on curved surfaces. (a) Circular Cone. (b) Circular Paraboloid.

Geodesics for the paraboloid is analyzed in cylindrical coordinates (ρ, ϕ, z) .

$$x = \rho \cos \phi, \quad y = \rho \sin \phi, \quad z = q + \rho^2$$

The resulting Jacobian and covariant unitary vectors are from (3.7.2).

$$\begin{pmatrix} \frac{\partial x}{\partial \rho} & \frac{\partial y}{\partial \rho} & \frac{\partial z}{\partial \rho} \\ \frac{\partial x}{\partial \phi} & \frac{\partial y}{\partial \phi} & \frac{\partial z}{\partial \phi} \\ \frac{\partial x}{\partial q} & \frac{\partial y}{\partial q} & \frac{\partial z}{\partial q} \end{pmatrix} = \begin{pmatrix} \cos \phi & \sin \phi & 2\rho \\ -\rho \sin \phi & \rho \cos \phi & 0 \\ 0 & 0 & 1 \end{pmatrix} \begin{matrix} \rightarrow \mathbf{E}_\rho \\ \rightarrow \mathbf{E}_\phi \\ \rightarrow \mathbf{E}_q \end{matrix} \quad (7.3.12)$$

The covariant metric coefficients follow from (3.x.x).

$$\begin{pmatrix} \mathbf{E}_\rho \cdot \mathbf{E}_\rho = g_{\rho\rho} & \mathbf{E}_\rho \cdot \mathbf{E}_\phi = g_{\rho\phi} & \mathbf{E}_\rho \cdot \mathbf{E}_q = g_{\rho q} \\ & \mathbf{E}_\phi \cdot \mathbf{E}_\phi = g_{\phi\phi} & \mathbf{E}_\phi \cdot \mathbf{E}_q = g_{\phi q} \\ & & \mathbf{E}_q \cdot \mathbf{E}_q = g_{qq} \end{pmatrix} = \begin{pmatrix} 1+4\rho^2 & 0 & 2\rho \\ 0 & \rho^2 & 0 \\ 2\rho & 0 & 1 \end{pmatrix} \quad (7.3.13)$$

This gives a kinetic energy and (for $V=0$) a Lagrangian. We constrain the q -terms in braces $\{\}$ to zero.

$$T = L = \frac{1}{2} \gamma_{\mu\nu} \dot{q}^\mu \dot{q}^\nu = \frac{m}{2} (1+4\rho^2) \dot{\rho}^2 + \frac{m}{2} \rho^2 \dot{\phi}^2 + \frac{m}{2} \{2\rho \dot{q} \dot{\phi} + \dot{q}^2\} \quad (7.3.14)$$

Two canonical momenta p_ρ and p_ϕ are left. Cylindrical symmetry conserves azimuthal momentum $p_\phi = \ell$. Also, Hamiltonian $T=H$ is conserved ($H=\epsilon$) since it has no explicit time dependence.

$$T = L = H = \frac{m}{2} (1+4\rho^2) \dot{\rho}^2 + \frac{\ell^2}{2m\rho^2} = \epsilon = \text{const.} \quad (7.3.15a)$$

$$\text{where: } p_\rho = \frac{\partial L}{\partial \dot{\rho}} = m(1+4\rho^2) \dot{\rho} \quad (7.3.15b) \quad p_\phi = \frac{\partial L}{\partial \dot{\phi}} = m\rho^2 \dot{\phi} = \ell = \text{const.} \quad (7.3.15c)$$

Radial momentum varies according to Lagrange-Riemann equations

$$\dot{p}_\rho = m(1+4\rho^2) \ddot{\rho} + 8m\rho \dot{\rho} = \frac{\partial L}{\partial \rho} = 4m\rho \dot{\rho}^2 - \frac{\ell^2}{m\rho^3} \quad (7.3.16)$$

The direct quadrature integral solution of (7.3.15a) is the following.

$$\int \rho d\rho \frac{\sqrt{1+4\rho^2}}{\sqrt{\frac{2\epsilon}{m} \rho^2 - \frac{\ell^2}{m^2}}} = \int dt$$

(b) Tautochrone-brachistichone curves

Perhaps no minimization problem is older or more famous than the *brachistichone* or minimum-time curve for a particle falling in a uniform gravitational potential. Its solution is the same as that of another problem, the *tautochrone* or equal-time period curve which Huygens sought for much of his life. Energy conservation gives velocity v from gravitational g .

$$\frac{ds}{dt} = v = \sqrt{2gy} \quad (7.3.17a)$$

The elapsed travel time which we seek to minimize is the following.

$$t = \int dt = \int \frac{ds}{\sqrt{2gy}} = \int dx \frac{\sqrt{1+y'^2}}{\sqrt{2gy}} = \int dy \frac{\sqrt{1+x'^2}}{\sqrt{2gy}} \tag{7.3.17b}$$

Let us try *Solution 4* of (7.2.11) ; a pseudo-momentum p_x for a y -integral which has no x dependence.

$$p_x = const. = \frac{\partial}{\partial x'} \frac{\sqrt{1+x'^2}}{\sqrt{2gy}}, \quad \text{where: } x' = \frac{dx}{dy} = \frac{1}{y'} \tag{7.3.18a}$$

$$= \frac{x'}{\sqrt{1+x'^2} \sqrt{2gy}} = \frac{1}{\sqrt{y'^2+1} \sqrt{2gy}}$$

Changing variables from y to velocity v using (7.3.17) simplifies the equation.

$$v^2 = 2gy, \quad dy = \frac{v dv}{g}, \quad y' = \frac{v}{g} \frac{dv}{dx} \tag{7.3.18b}$$

$$p_x^2 \left(\frac{v^2}{g^2} + 1 \right) 2gy = 1 = \left(\frac{p_x v^2}{g} \frac{dv}{dx} \right)^2 + p_x^2 v^2 \tag{7.3.18c}$$

An elementary integral results and suggests an elementary substitution $v = a \cos\theta$.

$$\int \frac{v^2 dv}{g\sqrt{a^2 - v^2}} = \int dx, \quad \text{where: } a^2 = 1/p_x^2 \tag{7.3.19}$$

Setting $v = a \cos\theta$ immediately yields solutions for both x and y in terms of an angle parameter θ .

$$v^2 = 2gy = a^2 \cos^2 \theta, \quad dv = -a \sin \theta d\theta$$

$$y = \frac{a^2}{2g} \cos^2 \theta, \quad x = -\int \frac{a^2}{g} \cos^2 \theta d\theta = -\int \frac{a^2}{2g} (1 + \cos 2\theta) d\theta \tag{7.3.20}$$

$$y = R(1 + \cos 2\theta), \quad x = -R(2\theta + \sin 2\theta) \quad \text{where: } R = \frac{a^2}{4g}$$

The result (7.3.20) is a *cycloid* made by a point on a wheel rolling on a ceiling as shown in Fig. 7.3.3.

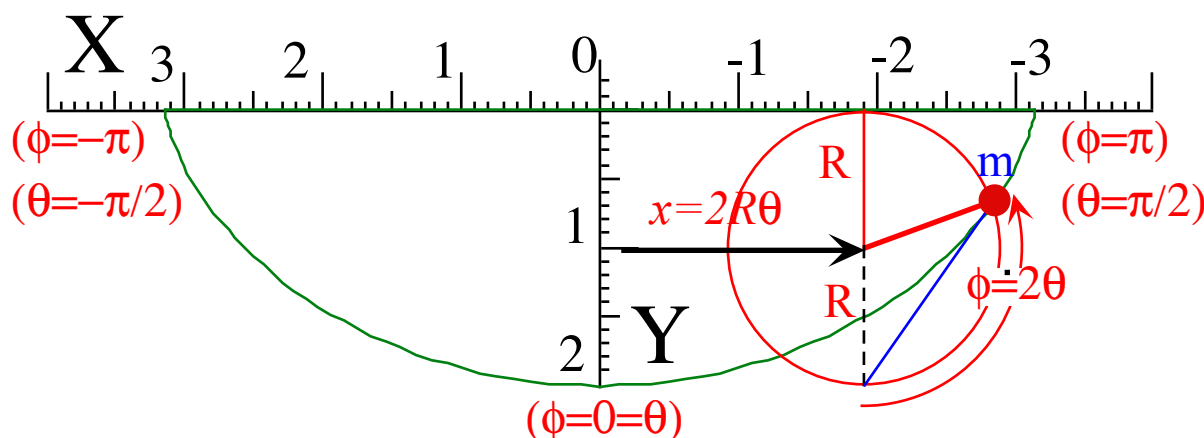


Fig. 7.3.3 Right cycloid generated by a circle rolling below $y=0$.

The angle $\phi = 2\theta$ of wheel rotation is positive (counter-clockwise) in Fig. 7.3.3 so the wheel contact point on the ceiling line $y=0$ translates right by $x = -R\phi$ along the line as the wheel rolls without slipping on it. (The coordinate system suggested by (7.3.20) is inverted; $+X$ is to the left and $+Y$ is down.)

Some extraordinary properties of the cycloid (7.3.20) are due to the invariant p_x in (7.3.18a).

$$\frac{1}{p_x^2} = \text{const.} = 2gy(y'^2 + 1) = v^2 \sec^2 \theta = a^2 \tag{7.3.21}$$

Here $v = a \cos \theta$ was used again. Rewriting velocity v using time derivatives yields an expression.

$$v^2 = \dot{x}^2 + \dot{y}^2 = \dot{\phi}^2 \left[(R + R \cos \phi)^2 + (-R \sin \phi)^2 \right] = 2R\dot{\phi}^2 (1 + \cos \phi) = 4R^2 \dot{\phi}^2 \cos^2 \theta \tag{7.3.22}$$

Comparing this to $v = a \cos \theta$ leads to the remarkable result that the circle turns at a constant angular frequency $\dot{\phi} = \omega$ and rolls along at a constant linear velocity ωR . (See Exercise 3.8.1.)

$$\frac{1}{p_x} = a = \sqrt{4gR} = 4R\dot{\phi} = 8R\dot{\theta}, \quad \text{or: } \omega = \dot{\phi} = \sqrt{\frac{g}{4R}} \tag{7.3.23}$$

This in turn gives a simple formula for the arc length of the cycloid from bottom ($\theta = 0$) to angle $\theta < \pi/2$.

$$s = \int_0^t v dt = \int_0^\theta 4R\omega \cos \theta dt = \int_0^\theta 4R(\omega / \dot{\theta}) \cos \theta d\theta = 4R \sin \theta \tag{7.3.24}$$

Arc length s is indicated by a segment hh of length $2h = 4R \sin \theta$ in Fig. 7.3.4.

(c) Huygen's pendulum

Note the segment hh between points m' and m'' acts like a flexible wire attached to an ascending point m'' and tangent to its cycloid as shown in the upper right hand portion of Fig. 7.3.4. The hh wire is unwinding from the m'' cycloid while its descending end-point m' generates another similar cycloid curve. The tangent to the m' cycloid, in turn, is a similar wire segment $h'h'$ of length $2h' = 4R \cos \theta$ which is attached to the original mass point m and winding onto the m' cycloid as shown in the bottom right hand portion of Fig. 7.3.4. This generates the original m cycloid as points m and m'' execute identical motions and take turns with the point m' . (When m and m'' are near the top of their cycloid m' is near its bottom and *vice-versa*.) Total top-to-bottom arc length is $4R$ according to (7.3.24) and holds for each cycloid.

The segment hh is the *radius of curvature* $r_c(m') = 2h = 4R \sin \theta$ of the m' cycloid and the points m' or m'' are *centers of curvature* for circular arcs around unwinding points m'' or m' , respectively. Segment $h'h'$ is the radius of curvature $r_c(m) = 2h' = 4R \cos \theta$ of the m cycloid whose center of curvature is at the point m' . The three wheels roll synchronically on their ceilings. As point m approaches the top of a cycloid point m' approaches m so that curvature becomes infinite. ($k = 1/r_c \rightarrow \infty$ as $\theta \rightarrow \pi/2$.)

Fig. 7.3.4 shows examples of circular arcs fitting a cycloid. The largest arc and one with the least curvature $k_c = 1/(4R)$ is a circle of radius $r_c = 4R$ that surrounds the entire cycloid. This is the path of a simple circular pendulum. The figure shows that the circle deviates only slightly from the cycloid with the greatest deviation near the tips of the cycloid where curvature blows up.

The constructions sketched in Fig. 7.3.4 are part of what is known as a *Huygen's pendulum*. The cycloid pendulum represents one of the great achievements of a preeminent 17th century physicist, Christian Huygens who spent much of his life trying to improve the quality of astronomical pendulum clocks. The use of a cycloid to "pinch" the fulcrum was only realized late in Huygen's lifetime. Before that he had achieved considerable improvement using a pair of circles; not a bad approximation as we have noted.

The cycloid path has the unique ability to guarantee the same frequency $\omega = \sqrt{g/4R}$ for any amplitude θ_0 of oscillation within the range $\{-\pi/2 < \theta_0 < \pi/2\}$ between cycloid tips. The circular pendulum frequency $\omega = \sqrt{g/l}$ holds for small amplitudes $\theta \ll 1$ but degrades at large amplitudes. The time integral (7.3.17b) is modified for arbitrary $\theta_0 \{-\pi/2 < \theta_0 < \pi/2\}$.

$$t_{1/4} = \int_{s_0}^0 \frac{ds}{\sqrt{2g(y-y_0)}} = \int_0^{\theta_0} \frac{4R \cos \theta d\theta}{\sqrt{2gR(\cos 2\theta - \cos 2\theta_0)}} = \sqrt{\frac{4R}{g}} \int_0^{\theta_0} \frac{\cos \theta d\theta}{\sqrt{\sin^2 \theta_0 - \sin^2 \theta}} \quad (7.3.25a)$$

Arc length $s=4R \sin \theta$ (7.3.24) and cycloid height $y=R(1+\cos 2\theta)$ are used. Let: $\sin \theta = \sin \theta_0 \sin \alpha$.

$$t_{1/4} = \sqrt{\frac{4R}{g}} \int_0^{\alpha=\pi/2} \frac{\sin \theta_0 \cos \alpha d\alpha}{\sin \theta_0 \sqrt{1 - \sin^2 \alpha}} = \frac{\pi}{2} \sqrt{\frac{4R}{g}} \quad (7.3.25b)$$

A cycloid has a full period of $t_I = 2\pi\sqrt{\ell/g}$ for all θ_0 . It matches a simple ($\ell=4R$)-pendulum for $\theta_0 \ll 1$.

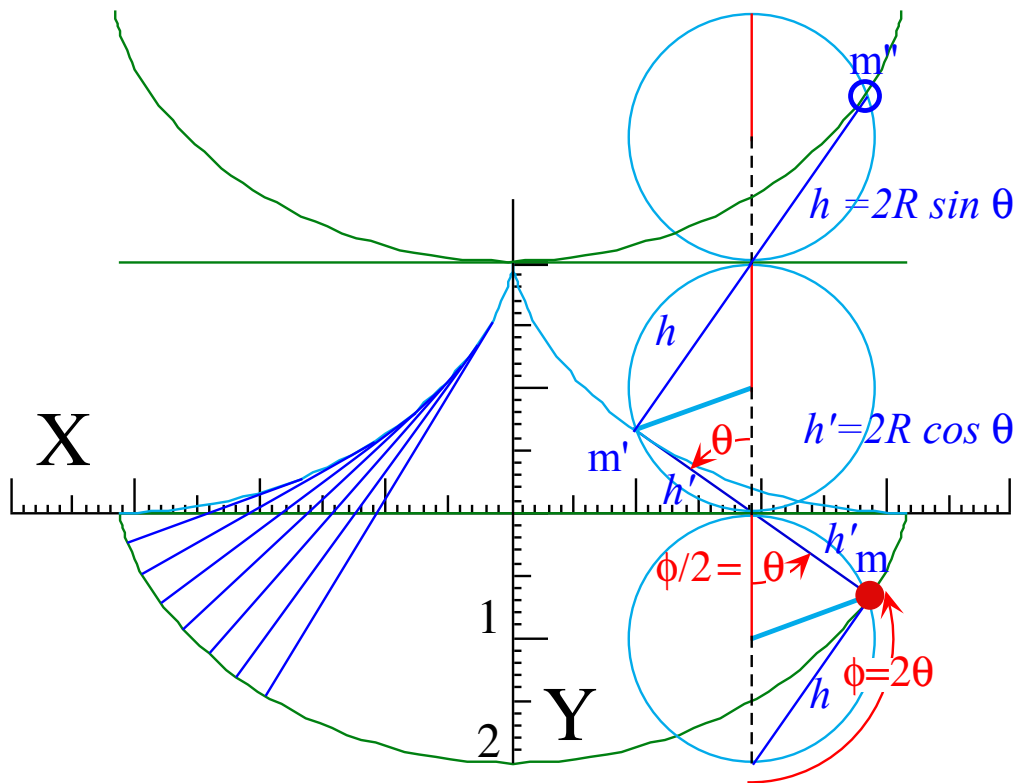


Fig. 7.3.4 Cycloid paths generated by a wires unwinding from similar cycloids.

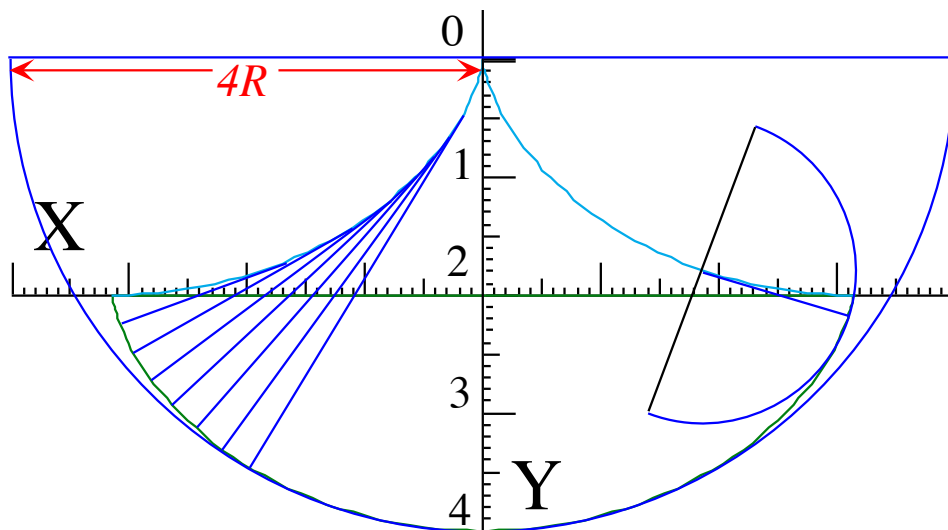


Fig. 7.3.5 Cycloid path of Huygen's pendulum compared to that of simple circular pendulum.

Chapter 7.4 Curve Families and Contact Relations

The following begins with a review of functional optimization and contact relations introduced in Ch. 12 of Unit 1. The example used there and sketched again below is an ancient artillery problem: What launch angle α gives maximum range? Nowadays high-speed computers let us optimize functions of many variables using a "brute-force" or "Monte-Carlo" approach of trial and error as sketched in Fig. 7.4.1 below that tries over sixty values of angle α between 0° and 360° . This is an example of a *family of trajectories* or *curve family*.

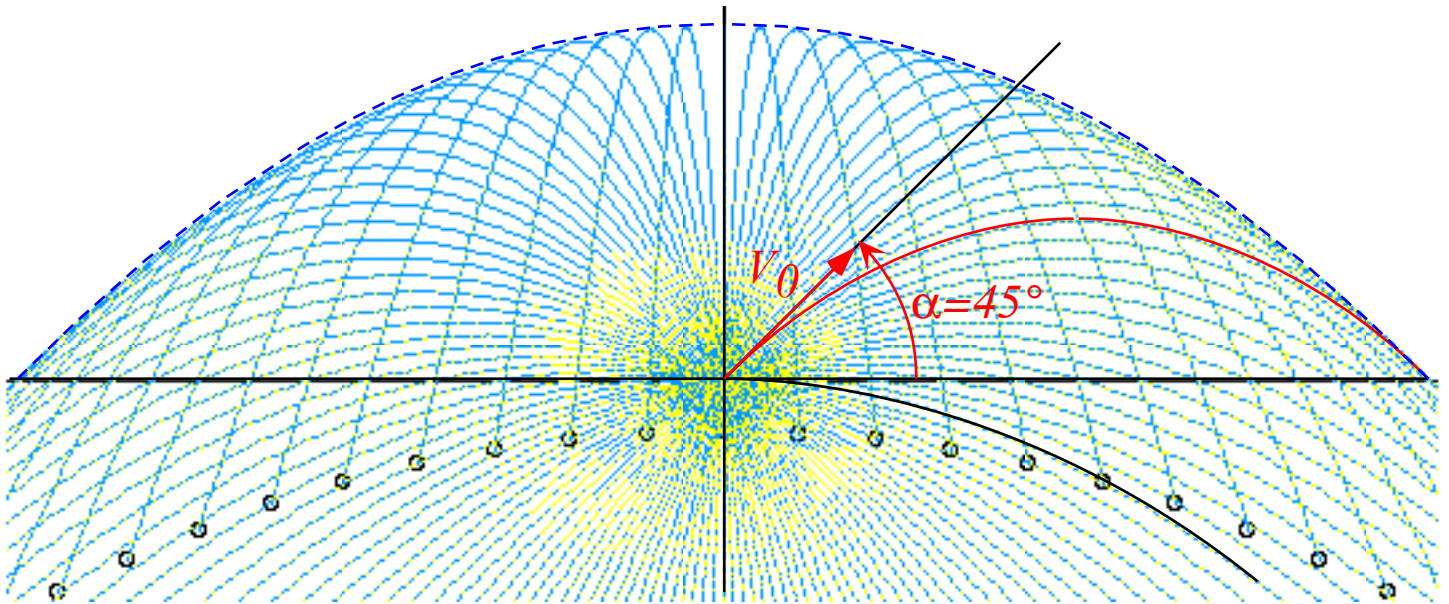


Fig. 7.4.1 Family of trajectories with fixed initial velocity v_0 and varying launch angle α .

Each of the curves share something in common (Here all have the same initial v_0 .) while differing in other ways. (Here the distinguishing variable is initial angle α of launch.) A key feature of Fig. 7.4.1 is the dashed enveloping arch or *contacting envelope function* of the curve family of solutions $\mathbf{x}(t) = (x(t), y(t))$ to the elementary trajectory equation $\ddot{\mathbf{x}} = -\mathbf{g}$ for constant gravity $\mathbf{g} = -g\mathbf{e}_y$.

The initial conditions of position are $x(0) = 0 = y(0)$ while initial velocity components are as follows

$$\dot{x}(0) = v_x(0) = v_0 \cos \alpha, \quad \dot{y}(0) = v_y(0) = v_0 \sin \alpha. \quad (7.4.1)$$

The time solutions are the integrals of the trajectory equation $(\ddot{x}, \ddot{y}) = (0, -g)$ subject to initial values.

$$x(t) = (v_0 \cos \alpha)t, \quad y(t) = (v_0 \sin \alpha)t - \frac{1}{2}gt^2. \quad (7.4.2)$$

Eliminate time $t = x/(v_0 \cos \alpha)$ using the x -solution. An individual trajectory $y(x)$ curve function results.

$$y(x) = \frac{v_0 \sin \alpha}{v_0 \cos \alpha} x - \frac{gx^2}{2v_0^2 \cos^2 \alpha}. \quad (7.4.3)$$

Each trajectory is the zero value of a *Contact Generating Function* $S(v_0, \alpha : x, y)$ as follows.

$$S(v_0, \alpha : x, y) = -y + x \tan \alpha - \frac{gx^2}{2v_0^2 \cos^2 \alpha} = 0. \quad (7.4.4)$$

In other words, $S(v_0, \alpha : x, y)$ maps each initial value point (v_0, α) in Fig. 7.4.2 onto a complete trajectory curve $y(x)$. A horizontal line of points (same v_0 but differing α) gives the v_0 -family of trajectories.

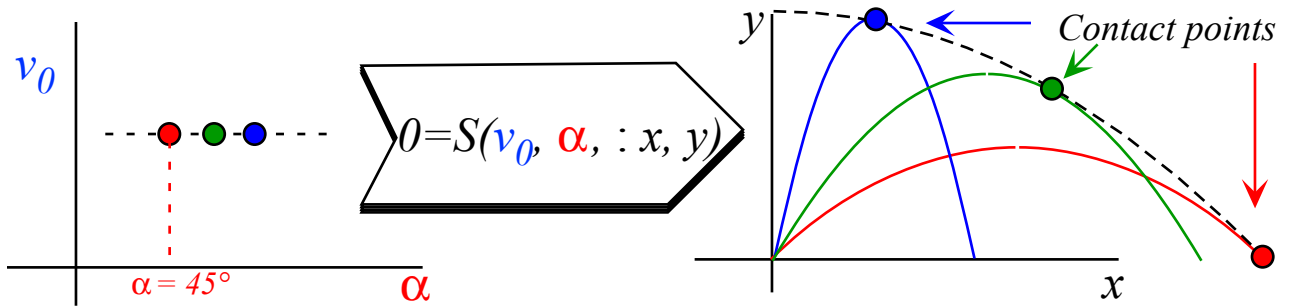


Fig. 7.4.2 Generating function maps trajectories with fixed initial velocity v_0 and varying launch angle α .

The contact points between the individual family member trajectories and their family boundary represent a kind of extreme. Contact points are where the generating function value is least sensitive to a change in the angle α . More precisely, they are points of zero first α -derivative; no first-order change.

$$\frac{\partial S(v_0, \alpha : x, y)}{\partial \alpha} = 0 \tag{7.4.5a}$$

$$x \frac{\partial \tan \alpha}{\partial \alpha} - \frac{gx^2}{2v_0^2} \frac{\partial \cos^{-2} \alpha}{\partial \alpha} = 0 = \frac{x}{\cos^2 \alpha} - \frac{gx^2}{2v_0^2} \frac{2 \sin \alpha}{\cos^3 \alpha} \tag{7.4.5b}$$

Solving this equation relates the x -value and the α -value of each contact point for a given v_0 .

$$\tan \alpha = \frac{v_0^2}{gx}, \quad \text{or:} \quad x = \frac{v_0^2}{g \tan \alpha} . \tag{7.4.5b}$$

Substitution of this relation into generating function (7.4.4) yields a contact envelope function.

$$y(x) = x \tan \alpha - \frac{gx^2}{2v_0^2} (1 + \tan^2 \alpha) \Rightarrow y(x) = x \frac{v_0^2}{gx} - \frac{gx^2}{2v_0^2} \left(1 + \frac{v_0^4}{g^2 x^2} \right) \tag{7.4.6}$$

$$= \frac{v_0^2}{2g} - \frac{gx^2}{2v_0^2}$$

This is the dashed parabolic curve contacting all parabolic family curves in Fig. 7.4.1 and Fig. 7.4.2.

Coincidentally, it also has the shape of the ($\alpha = 0$)-trajectory that is sketched in Fig. 7.4.1. Often a contact function for a family of trajectories is itself a possible trajectory though usually not actually a family member.

(a) Contact transformations

The transformation shown in Fig. 7.4.2 of a line in (v_0, α) -space to a curve in (x,y) -space is an example of a *contact transformation*. A generic contact transformation is indicated in Fig. 7.4.3 below.

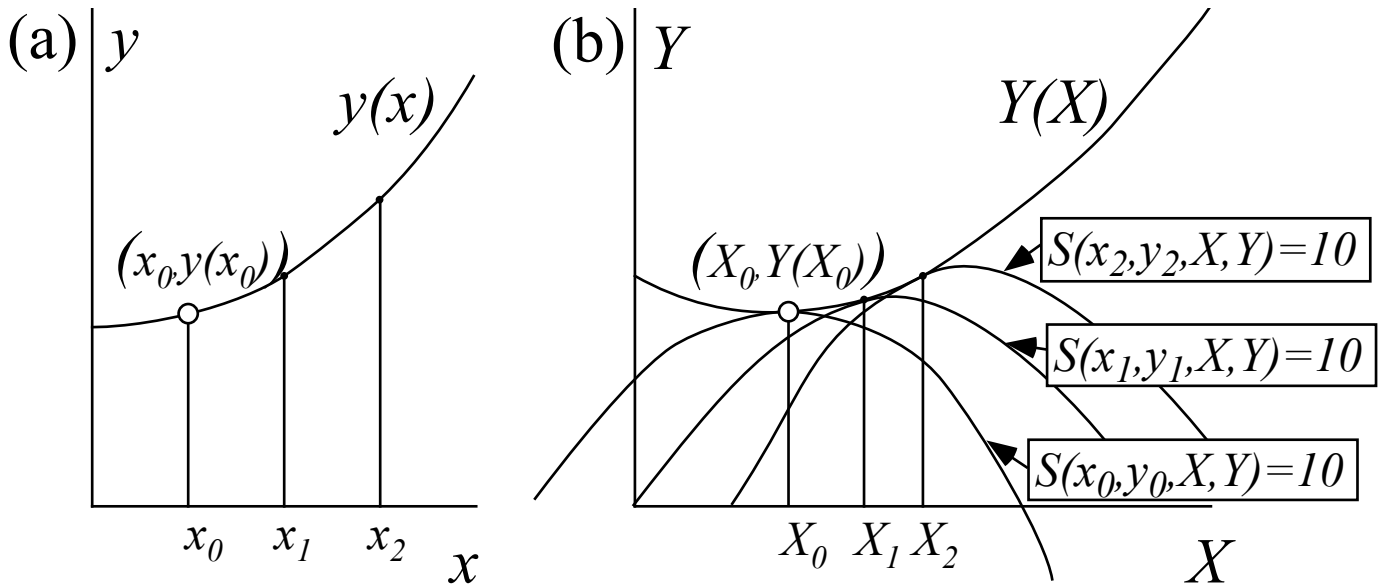


Fig. 7.4.3 Geometry of a general contact transformation $y(x) \rightarrow Y(X)$.

As in Fig. 7.4.2 there is one curve $S(x,y : X,Y) = const.$ in the XY -space for each point (x,y) on the curve $y(x)$ in xy -space. The envelope(s) or contacting curve(s) $Y(X)$ are the desired contact transformation of the curve $y(x)$.

Each point $(x_0, y(x_0))$ is mapped onto a contact point $(X_0, Y(X_0))$ in the XY -space. At such points, the values of the generator $S(x,y : X,Y)$ are least sensitive to changing the original point x_0 . In Fig. 7.4.3, a small change in x_0 causes the $S = const.$ curve to slide a little along the $Y(X)$ envelope but this does not cause the contact point $(X_0, Y(X_0))$ to stray from the sliding curve, at least at first. Hence, to first order

$$\left. \frac{\partial S(x, y(x) : X, Y)}{\partial x} \right|_{x=x_0} = 0. \tag{7.4.7a}$$

Note that contact transformations are a two-way deal; each point $(X_0, Y(X_0))$ generates a tangent curve (not shown in Fig. 7.4.3a) to the $y(x)$ curve at $(x_0, y(x_0))$, and the following equation is applicable, too.

$$\left. \frac{\partial S(x, y : X, Y(X))}{\partial X} \right|_{X=X_0} = 0 \tag{7.4.7b}$$

(b) Legendre transformations

One kind of contact transformation is a *Legendre transformation* which uses straight lines, rather than curves, to contact its envelopes. (Recall in Sec. 1.12.) This is depicted in Fig. 7.4.4. Each xy -point $(x_j, y(x_j))$ maps to a line in XY -space with slope x_j and Y -intercept $-y_j$ as generated by relation

$$S(x,y : X,Y) = y + Y - xX = 0. \tag{7.4.8}$$

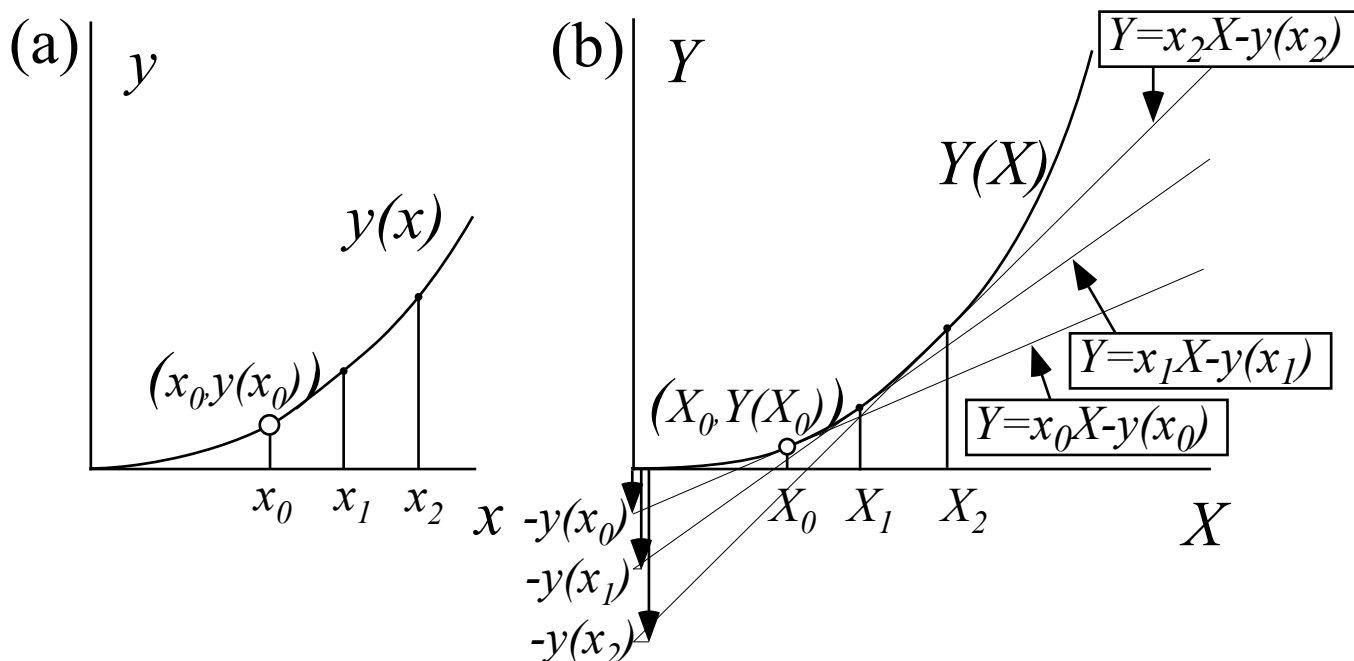


Fig. 7.4.4 Geometry of a Legendre contact transformation $y(x) \rightarrow Y(X)$.

Derivative relations (7.4.7) combine with the generator to locate contact points.

$$Y = xX - y \text{ where: } \frac{\partial S}{\partial x} = 0 \Rightarrow X = \frac{\partial y}{\partial x}, \text{ and } \frac{\partial S}{\partial X} = 0 \Rightarrow x = \frac{\partial Y}{\partial X} \quad (7.4.9)$$

Legendre transformation between Lagrangian $y(x) = L(\dot{q})$ and Hamiltonian $Y(X) = H(p)$ is as follows.

$$H = \dot{q}p - L \text{ where: } \frac{\partial S}{\partial \dot{q}} = 0 \Rightarrow p = \frac{\partial L}{\partial \dot{q}}, \text{ and } \frac{\partial S}{\partial p} = 0 \Rightarrow \dot{q} = \frac{\partial H}{\partial p} \quad (7.4.10)$$

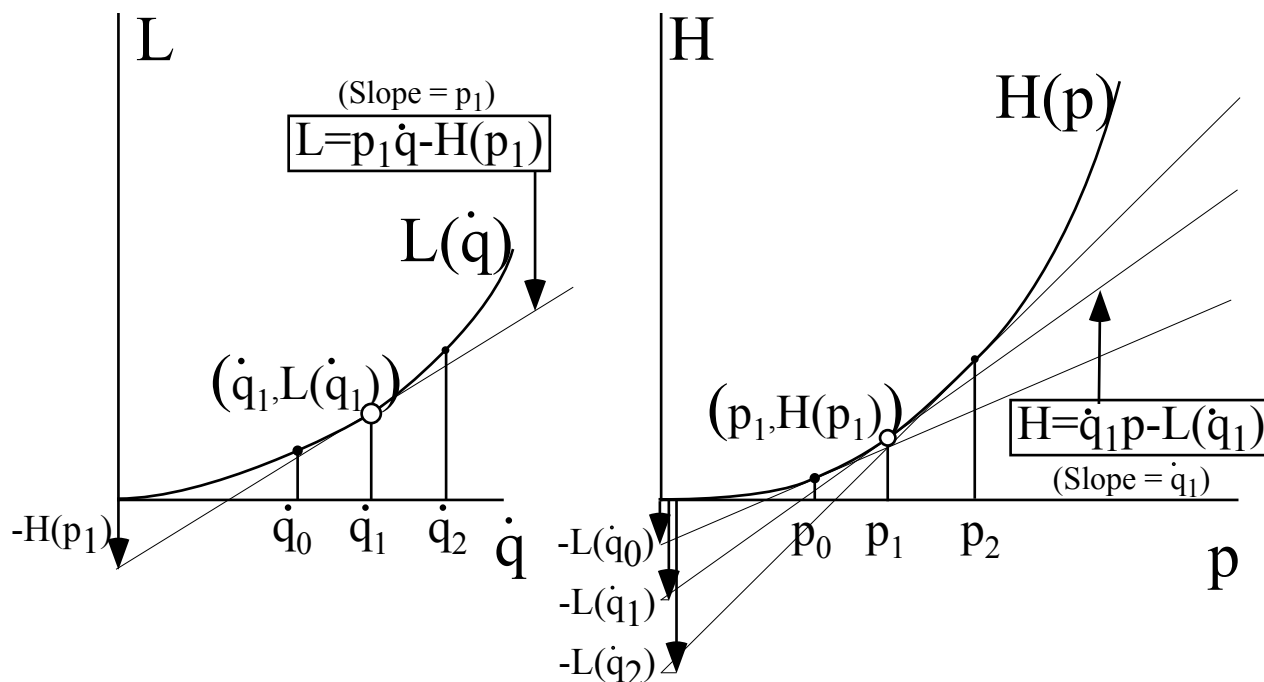


Fig. 7.4.5 Geometry of a Legendre transformation of Lagrangian L to Hamiltonian H .

The slope of the H versus p curve is the velocity \dot{q} in agreement with Hamilton's equations. In quantum theory, the Hamiltonian or energy $E=H$ corresponds to frequency ($E=\hbar\omega$ by Planck's axiom.) while momentum p corresponds to wavevector ($p=\hbar k$ by DeBroglie's formula.) An ω versus k curve is called a *dispersion function* and its slope or derivative $\frac{d\omega}{dk}$ is the wave group velocity

$$\frac{d\omega}{dk} = V_{group}. \quad (7.4.11)$$

V_{group} is also the classical particle velocity \dot{q} according to the preceding relations. On the other side of Fig. 7.4.5, the slope p of the Lagrangian curve is inversely related to the wave phase velocity

$$V_{phase} = \omega / k. \quad (7.4.12)$$

Note that the Legendre transformation of the Lagrangian and the Hamiltonian has the form of the Poincare' relation first seen in Chapter 1 (equation (1.12.11)) Chapter 2 (equation (2.6.9b)) and in Chapter 3 (equation (3.8.5)).

$$L = p \dot{q} - H, \text{ or:} \quad H = p \dot{q} - L$$

For multiple coordinate dimensions it takes the generalized coordinate form.

$$L = p_m \dot{q}^m - H, \text{ or:} \quad H = p_m \dot{q}^m - L$$

The effect of the other dimensions on Fig. 7.4.5 is simply to move the position of the intercept origin downward or, equivalently, shift the contacting curves upward.

Chapter 7.5 Action: Generators of Active Contact Transformations

The Hamilton principle action S_p can be viewed as a bi-variant functional $S_p(\mathbf{r}_0, t_0 : \mathbf{r}_1, t_1)$ of an initial space-time point (\mathbf{r}_0, t_0) and a final space-time point (\mathbf{r}_1, t_1) as well as the $\mathbf{r}(t)$ between them.

$$S_p(\mathbf{r}_0, t_0 : \mathbf{r}_1, t_1) = \int_{t_0}^{t_1} dt L(\mathbf{r}(t), \dot{\mathbf{r}}(t), t) \tag{7.5.1}$$

As such, it is the generating function of the contact transformation to end all contact transformations; it is the prime mover of the entire classical mechanical universe! Given (\mathbf{r}_0, t_0) one finds (\mathbf{r}_1, t_1) .

It is customary to distinguish *active transformations*, that is, ones which move or change the state of actual physical objects, from *passive transformations*, that is, ones which merely re-label an object or state without actually changing it. If so, then a transformation of a system from one point (\mathbf{r}_0, t_0) in space-time to another point (\mathbf{r}_1, t_1) (presumably later but not necessarily so!) is definitely an active one. The contact transformation generated by $S_p(\mathbf{r}_0, t_0 : \mathbf{r}_1, t_1)$ certainly is active, and so, perhaps, this is the reason we call the active generating function S_p by the name *action*.

Later, we shall consider other generating functions, usually labeled by the letter F , which generate passive or change-of-variable transformations. Legendre transformation is an example. A passive generator merely dresses up physics in different clothing, so one might see F called *fashion* or *passion* if classical mechanics had a sense of humor. Unfortunately, they usually don't so one usually won't.

(a) Hamilton's characteristic action

A second type of action is known as *Hamilton's characteristic action* S_H or *reduced action*.

$$S_H(\mathbf{r}_0 : \mathbf{r}_1) = \int_{\mathbf{r}_0}^{\mathbf{r}_1} \mathbf{p} \bullet d\mathbf{r} \tag{7.5.2a}$$

Reduced action is a spatial integral of phase-space area $p_m dq^m = p_m \dot{q}^m dt$ and a time integral of the sum of the Hamiltonian H and Lagrangian L according to the Poincare' relation $L dt = p_m dq^m - H dt$.

$$S_H(\mathbf{r}_0 : \mathbf{r}_1) = \int_{t_0}^{t_1} \mathbf{p} \bullet \dot{\mathbf{r}} dt = \int_{t_0}^{t_1} (H + L) dt = 2 \int_{t_0}^{t_1} T dt \tag{7.5.2b}$$

The final integral over kinetic energy T results if the Hamiltonian can be written $H=T+V$ so it cancels the potential V in the Lagrangian $L=T-V$. Poincare' relation between the actions S_p and S_H is given.

$$\begin{aligned} S_p(\mathbf{r}_0, t_0 : \mathbf{r}_1, t_1) &= \int_{\mathbf{r}_0}^{\mathbf{r}_1} \mathbf{p} \bullet d\mathbf{r} - \int_{t_0}^{t_1} dt H \\ &= S_H(\mathbf{r}_0 : \mathbf{r}_1) - (t_1 - t_0) E \quad (\text{for: } H = E = \text{const.}) \end{aligned} \tag{7.5.3}$$

A Hamiltonian with no explicit t -dependence is a constant of motion as given in the last line. Then the two kinds of action differ only by a product of energy and elapsed time. Variation of functional S_H is done by fixing total energy E and varying only the spatial trajectory path $y(x)$ between its end points \mathbf{r}_0 and \mathbf{r}_1 as sketched in Fig. 7.5.1. Keeping E fixed makes time end point t_1 vary with different paths..

Imagine that path \mathbf{r} or $y(x)$ is a flexible frictionless tube whose shape is bent to $y(x)+\Delta\psi(x)$ or $\mathbf{r}+\Delta\mathbf{r}$ in Fig. 7.5.1. With each variation function $\Delta y(x)$ the particle is shot with energy E into the \mathbf{r}_0 end and forced

(Constrained is a better word, perhaps!) to go along a new tube but come out at the same x_I end point. Since E is constrained to be constant, different paths may have different travel times $t_I + \Delta t$ as indicated in Fig. 7.5.1. Compare to Fig. 7.3.1 in which the particle is constrained *and forced* to finish at the same time with each variation δy .

We ask, "What is special about a *natural* path (or paths), that is, a path \mathbf{r} or $y(x)$ which happens on its own without needing a flexible tube to constrain its journey from \mathbf{r}_0 to \mathbf{r}_I ?"

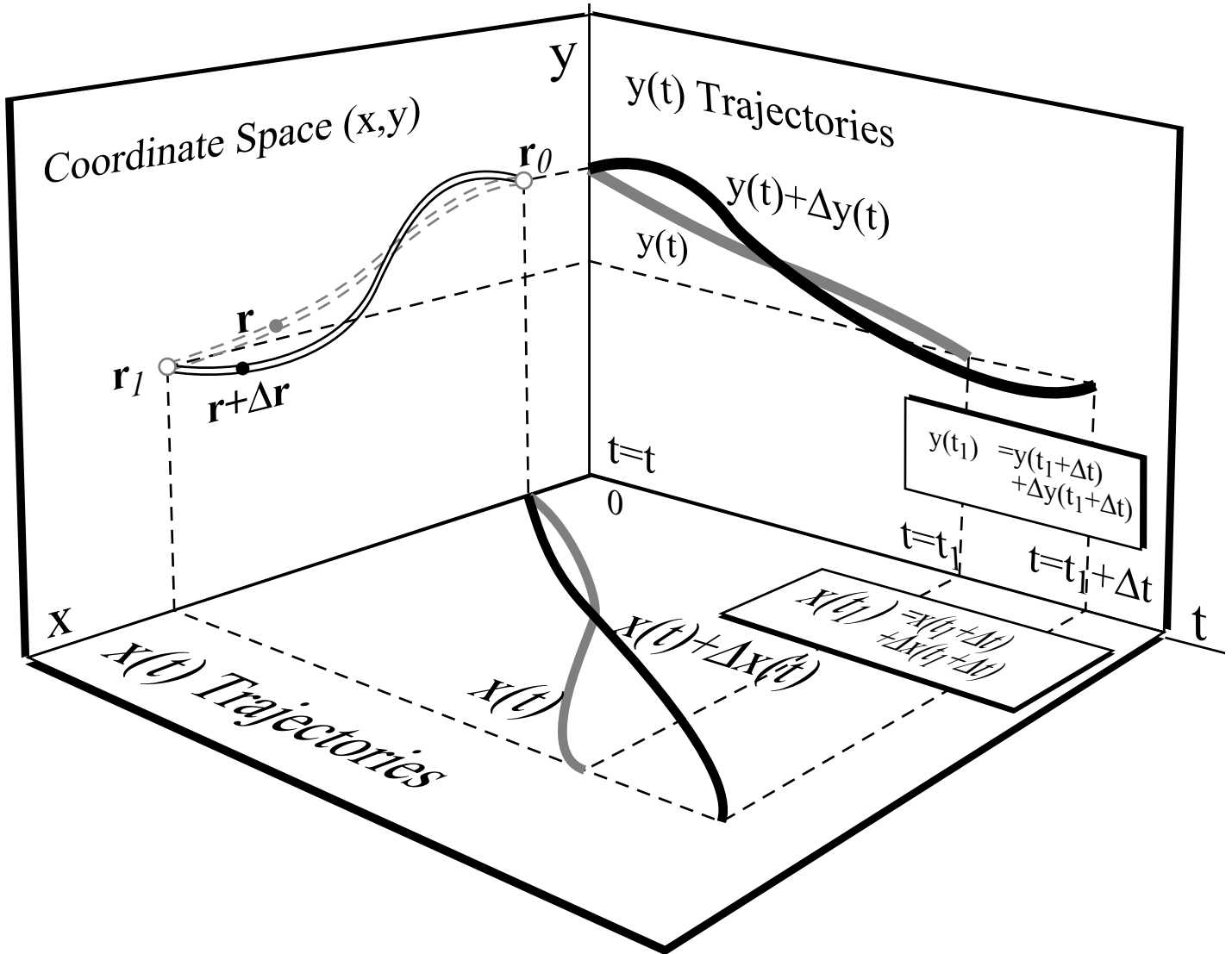


Fig. 7.5.1 Variation of paths and time trajectories for evaluating Hamilton's characteristic action S_H .

First order variation $\Delta S^{(1)}_H$ is like $\delta S^{(1)}_p$ in (7.3.5a) but it has extra terms for time "tardiness" Δt .

$$\begin{aligned} \Delta S^{(1)}_H &= S^{(1)}_H(q + \Delta q) - S_H(q) = \int_{t_0}^{t_1 + \Delta t} dt [L(q + \Delta q) + H(q + \Delta q)] - \int_{t_0}^{t_1} dt [L(q) + H(q)] \\ &= \int_{t_0}^{t_1} dt \left[\frac{\partial L}{\partial q^\mu} - \frac{d}{dt} \left(\frac{\partial L}{\partial \dot{q}^\mu} \right) \right] \Delta q^\mu + \frac{\partial L}{\partial \dot{q}^\mu} \Delta q^\mu (t_1) + H \Delta t + L \Delta t \end{aligned} \quad (7.5.4a)$$

The first-order approximation drops all second-order (or higher) terms such as $(\Delta q)^2$ or $\Delta q \Delta t$ or $(\Delta t)^2$. A parts term $\Delta q^\mu(t_1)$ does not vanish as it did in (7.3.2). Instead, as in Fig. 7.5.1, the following holds.

$$\begin{aligned} q^\mu(t_1) &= q^\mu(t_1 + \Delta t) + \Delta q^\mu(t_1 + \Delta t) \\ &\equiv q^\mu(t_1) + \frac{\partial q^\mu}{\partial t} \Delta t + \Delta q^\mu(t_1) + \dots \end{aligned}$$

or
$$\Delta q^\mu(t_1) \equiv -\frac{\partial q^\mu}{\partial t} \Delta t + \dots \equiv -\dot{q}^\mu \Delta t \tag{7.5.4b}$$

This gives zero first-order variation if Lagrange equations and the Poincare' identity hold.

$$\Delta S_H^{(1)} = \int_{t_0}^{t_1} dt \left[\frac{\partial L}{\partial q^\mu} - \frac{d}{dt} \left(\frac{\partial L}{\partial \dot{q}^\mu} \right) \right] \Delta q^\mu - \frac{\partial L}{\partial \dot{q}^\mu} \dot{q}^\mu \Delta t + H \Delta t + L \Delta t = 0 \tag{7.5.4c}$$

Thus action S_H is stationary like S_p (In fact, both are minimum.) for a naturally occurring path.

(b) Hamilton Jacobi equations

The Poincare' identity gives the following differential relation for actions S_p and S_H .

$$dS_p = L dt = p_m dq^m - H dt = dS_H - H dt \tag{7.5.5a}$$

Expressing this as a first differential with respect to coordinate and time end points gives

$$dS_p = \frac{\partial S_p}{\partial q^\mu} dq^\mu + \frac{\partial S_p}{\partial t} dt, \quad dS_H = \frac{\partial S_H}{\partial q^\mu} dq^\mu \tag{7.5.5b}$$

where

$$\frac{\partial S_p}{\partial q^\mu} = p_\mu = \frac{\partial S_H}{\partial q^\mu}, \tag{7.5.5c} \quad \frac{\partial S_p}{\partial t} = -H, \tag{7.5.5d}$$

lead to what are called the *time-dependent Hamilton-Jacobi equations*. This is certainly a most advanced and esoteric form of Newton's equations; it reduces to a non-linear partial differential equation.

$$-\frac{\partial S_p}{\partial t} = H(p_1, p_2, \dots; q^1, q^2, \dots) = H\left(\frac{\partial S_p}{\partial q^1}, \frac{\partial S_p}{\partial q^2}, \dots; q^1, q^2, \dots\right) \tag{7.5.5e}$$

The characteristic action S_H satisfies the following *time-independent Hamilton-Jacobi equation* .

$$const. = E = H(p_1, p_2, \dots; q^1, q^2, \dots) = H\left(\frac{\partial S_H}{\partial q^1}, \frac{\partial S_H}{\partial q^2}, \dots; q^1, q^2, \dots\right) \tag{7.5.5f}$$

Recall (7.5.3): $S_p = S_H - H t$ (7.5.5g) or: $S_H = S_p + H t$ (7.5.5h)

(c) Example of H-J equations: Elementary trajectories

A quick way to see both utility and limitations of Hamilton-Jacobi theory is to return to the simple trajectory problem which began in Sec. 7.4. It will be evident that its power is not in the derivation of solutions to equations of motion. Quite the opposite, H-J theory is most often practically useless for individual trajectory analysis even for the sophomoric example we will consider first. The job of trajectory analysis is best handled by ordinary differential equations of Newton, Lagrange, Riemann, Euler or Hamilton as described in Units 2-3. H-J equations are partial differential equations that only seem to make simple problems into difficult ones or difficult problems impossible!

Rather, the H-J equation is appropriate for organizing and exposing properties of various *families* of trajectories. Since quantum theory, due to its inherent uncertainty, forces us to deal with such families, one hopes H-J theory may relate classical mechanics to quantum wave mechanics.

Here the uniform gravitational trajectory Hamiltonian is

$$E = H = (p_x^2 + p_y^2)/2m + mgy. \quad (7.5.6)$$

The time-independent H-J equation is from (7.5.5e); the time-dependent H-J equation is from (7.5.5f).

$$\frac{1}{2m} \left[\left(\frac{\partial S_p}{\partial x} \right)^2 + \left(\frac{\partial S_p}{\partial y} \right)^2 \right] + mgy = -\frac{\partial S_p}{\partial t}, \quad \frac{1}{2m} \left[\left(\frac{\partial S_H}{\partial x} \right)^2 + \left(\frac{\partial S_H}{\partial y} \right)^2 \right] + mgy = E = \text{const.}$$

(7.5.7a)

(7.5.7b)

As is usual for partial differential equations, we attempt solution by *separation of variables*.

$$S_H(x,y) = s_x(x) + s_y(y) \quad (7.5.8a)$$

$$S_p(x,y,t) = s_x(x) + s_y(y) + s_t(t) \quad (7.5.8a)$$

The S_p separation is guaranteed by (7.5.5g) with $s_t(t) = -Ht$ if the S_H separation splits as follows.

$$\frac{-1}{2m} \left(\frac{ds_x(x)}{dx} \right)^2 + E = \frac{1}{2m} \left(\frac{ds_y(y)}{dy} \right)^2 + mgy \quad (7.5.9)$$

Isolation of independent variable x and y on the left and right, respectively, means either side is constant.

$$\frac{-1}{2m} \left(\frac{ds_x(x)}{dx} \right)^2 + E = \quad \epsilon_y = \frac{1}{2m} \left(\frac{ds_y(y)}{dy} \right)^2 + mgy = \text{const.} \quad (7.5.10a)$$

$$\epsilon_x = \frac{1}{2m} \left(\frac{ds_x(x)}{dx} \right)^2 \quad \text{where: } E = \epsilon_x + \epsilon_y \quad (7.5.10b)$$

This is an example of *classical separability* of a system into two dimensions or "normal modes" that do not share energy. Such separation is not guaranteed, but when it is possible it is a very important property and technique. For this problem, it recapitulates the old saw that rifle bullets fired horizontally or dropped vertically hit the ground simultaneously. (Actually, this is baloney unless you are on the moon! Aero-dynamic forces on a hundred-mile-per-hour objects are enormous, unpredictable, and capable of coupling dimensions x , and y as well as z .)

The separated ordinary differential equations (7.5.10) are solved by conventional integration.

$$s_x(x) = \sqrt{2m\epsilon_x} (x_1 - x_0) = m\dot{x}_0 (x_1 - x_0) \quad (7.5.11a)$$

$$s_y(y) = \frac{-1}{3m^2g} \left[2m(\epsilon_y - mgy) \right]^{\frac{3}{2}} \Bigg|_{y_0}^{y_1} = \frac{-m}{3g} \left[(\dot{y}_1)^3 - (\dot{y}_0)^3 \right] \quad (7.5.11a)$$

Here the conventional velocity-momentum-energy relations peculiar to this system are used.

$$p_x = m\dot{x} = (2m\epsilon_x)^{\frac{1}{2}} \quad (7.5.11c)$$

$$p_y = m\dot{y} = \left(2m \left[\epsilon_y - mgy \right] \right)^{\frac{1}{2}} \quad (7.5.11d)$$

Time-dependent action in terms of travel time $T = t_1 - t_0$ follows from (7.5.5.g) and the above.

$$S_p = S_H - ET = m\dot{x}_0(x_1 - x_0) - \frac{m}{3g} \left[(\dot{y}_1)^3 - (\dot{y}_0)^3 \right] - ET \quad (7.5.12)$$

The remainder of this discussion will revolve around rewriting the action in terms of different variables.

Doing this uses individual trajectory equations, something that tends to get lost in the H-J theory.

$$x_1(T) = x_0 + \dot{x}_0 T \quad (7.5.13a) \quad \dot{x}_1(T) = \dot{x}_0 \quad (7.5.13b)$$

$$y_1(T) = y_0 + \dot{y}_0 T - \frac{g}{2} T^2 \quad (7.5.13c) \quad \dot{y}_1(T) = \dot{y}_0 - gT \quad (7.5.13d)$$

Putting \dot{y}_1 from (7.5.13b) and energy E from (7.5.6) into (7.5.12)

$$\begin{aligned} S_p &= m\dot{x}_0(x_1 - x_0) - \frac{m}{3g} \left[(\dot{y}_0 - gT)^3 - (\dot{y}_0)^3 \right] - ET \\ &= m\dot{x}_0(x_1 - x_0) - \frac{m}{3g} \left[-3gT(\dot{y}_0)^2 + 3(gT)^2 \dot{y}_0 - (gT)^3 \right] - \frac{mT}{2} \left[(\dot{x}_0)^2 + (\dot{y}_0)^2 + 2g\dot{y}_0 \right] \\ &= m\dot{x}_0(x_1 - x_0) + \frac{mT(\dot{y}_0)^2}{2} - mgT^2 \dot{y}_0 + \frac{mg^2 T^3}{3} - \frac{mT(\dot{x}_0)^2}{2} - \frac{mT(\dot{y}_0)^2}{2} - mgT\dot{y}_0 \\ &= \frac{mT(\dot{x}_0)^2}{2} + \frac{mT(\dot{y}_0)^2}{2} - mgT^2 \dot{y}_0 + \frac{mg^2 T^3}{3} - mgT\dot{y}_0 \end{aligned} \quad (7.5.14)$$

The last step uses x -time solution (7.5.13a).

$$(x_1 - x_0) = T\dot{x}_0$$

Result (7.5.14) is explicitly a function of elapsed time T and initial coordinate and velocity values. It could be obtained by direct integration using the fundamental definition $S_p = \int L dt$ of action. However, such an expression lacks the functional dependence on initial and final coordinate and time values needed to make a true generating function $S_p(\mathbf{r}_0, t_0 : \mathbf{r}_1, t_1) = S_p(x_0, y_0, 0 : x_1, y_1, T)$. The x and y -time solutions (7.5.13) give velocity in terms of position interval $\mathbf{r}_1 - \mathbf{r}_0$ and time interval $T = t_1 - t_0$.

$$\dot{x}_0 = \frac{(x_1 - x_0)}{T}, \quad \dot{y}_0 = \frac{y_1 - y_0}{T} + \frac{g}{2} T$$

$$S_p = \frac{m(x_1 - x_0)^2}{2T} + \frac{m \left(y_1 - y_0 + \frac{g}{2} T^2 \right)^2}{2T} - mgT^2 \left(\frac{y_1 - y_0}{T} + \frac{g}{2} T \right) + \frac{mg^2 T^3}{3} - mgT\dot{y}_0$$

This expands to the following.

$S_p = \frac{m(x_1 - x_0)^2}{2T} + \frac{m(y_1 - y_0)^2}{2T} + \frac{mgT}{2}(y_1 - y_0) + m\frac{g^2 T^3}{8} - mgT(y_1 - y_0) - \frac{mg^2 T^3}{2} + \frac{mg^2 T^3}{3} - mgT\dot{y}_0$ Finally, there emerges a simplified time-dependent generating function S_p , the principle action.

$$S_p = \frac{m(x_1 - x_0)^2}{2T} + \frac{m(y_1 - y_0)^2}{2T} - \frac{mgT}{2}(y_1 - y_0) - \frac{mg^2 T^3}{24} - mgT\dot{y}_0 \quad (7.5.15)$$

It is instructive to check the partial and total time derivatives of the principle action S_p . According to the fundamental definition of $S_p = \int L dt$, its total derivative should equal the Lagrangian function.

$$\frac{dS_p(\mathbf{r}_0, 0 : \mathbf{r}_1(T), T)}{dT} = L \tag{7.5.16}$$

But, its partial derivative should equal the negative Hamiltonian according to the H-J equation (7.5.5d)

$$\frac{\partial S_p(\mathbf{r}_0, 0 : \mathbf{r}_1, T)}{\partial T} = -H \tag{7.5.17}$$

To check the total derivative we differentiate the expression (7.5.14) and compare using (7.5.13).

$$\begin{aligned} \frac{dS_p}{dT} &= \frac{m(\dot{x}_0)^2}{2} + \frac{m(\dot{y}_0)^2}{2} - 2mgT\dot{y}_0 + mg^2T^2 - mgy_0 \\ &= \frac{m(\dot{x}_1)^2}{2} + \frac{m(\dot{y}_1)^2}{2} - mgy_1 = L(\text{at time: } t_1 = T) \end{aligned} \tag{7.5.16}_{\text{example}}$$

To check the partial derivative we differentiate the expression (7.5.15) and compare using (7.5.13).

$$\begin{aligned} \frac{\partial S_p}{\partial T} &= -\frac{m(x_1 - x_0)^2}{2T^2} - \frac{m(y_1 - y_0)^2}{2T^2} - \frac{mg}{2}(y_1 + y_0) - \frac{mg^2T^2}{8} \\ &= -\frac{m(\dot{x}_0)^2}{2} - \frac{m(\dot{y}_0)^2}{2} - mgy_0 = -H(\text{at time: } t_0) = -H(\text{at time: } t_1) \end{aligned} \tag{7.5.17}_{\text{example}}$$

An expression similar to (7.5.15) for the characteristic action S_H is the following.

$$S_H = \frac{m(x_1 - x_0)^2}{T} + \frac{m(y_1 - y_0)^2}{T} + \frac{mg^2T^3}{12} \tag{7.5.18}$$

However, $S_H(x_0, y_0 : x_1, y_1)$ is supposed to be explicitly energy dependent and time independent. Usually there is not a convenient expression for time T in terms of total energy E and end points $(\mathbf{r}_0 : \mathbf{r}_1)$, and this makes elegant and concise analytic expressions of action difficult or impossible. Even for this sophomoric trajectory problem we have pages of algebra but still not a lot to show for it all!

Nevertheless, action $S_p = \int Ldt$ and $S_H = S_p + HT$ are quite easy to compute and graph numerically. One only has to follow trajectories of a given energy H and mark off values of action S_p or S_H obtained by integrating along each path. This method is not so dependent on the analytic and algebraic concerns.

(d) Example of H-J wavefronts: wave and particle velocity

A path integration technique for solving H-J equations is called the *method of characteristics*. It was developed to solve partial differential wave equations by integrating along characteristic *rays* or directions of wave propagation. For the example considered here the rays are particle trajectories, that is, families of parabolic trajectories of a given initial energy such as were sketched in Fig. 7.4.1. According to the time-independent H-J equation (7.5.5c) particle momentum is the gradient of S_H .

$$p_\mu = \frac{\partial S_H}{\partial q^\mu}, \quad \text{or:} \quad \mathbf{p} = \nabla S_H. \tag{7.5.19}$$

Examples of constant- S_H contours are shown in Fig. 7.5.2. They are constant-phase wavefronts for a time-independent H-J "wavefunction" solution. The constant- S_H contours are not to be confused with constant-time- T contours that are descending circles shown in Fig. 7.5.3.

Fig. 7.5.3 shows how a swarm of classical particles behaves in this situation, while Fig. 7.5.2 is closer to an ultimate reality by approximating what quantum matter-waves do in the same situation. Fig. 7.5.3 seems quite natural and simple to us since we are mostly live in a classical world. There a circle of particles uniformly expands at velocity $v_0=1$ m/s while uniformly accelerating downward at $g=1$ m/s². (The equivalence principle equates it to a constant v_0 -expansion in an inertial frame as viewed by someone on an elevator accelerating upward at g .)

As a result, the particles on the bottom of the circles in Fig. 7.5.3 always have a more negative velocity (by $-2v_0$) than the particles on top, though each and every particle has the same negative acceleration. At time $T=1$ in Fig. 7.5.3, the downward drift of the circle just matches its expansion rate v_0 , and the top particles stop rising and start falling.

The sequence of S_H contours or action wavefronts in Fig. 7.5.2 can also be viewed as a sequence in time, but it is different from the classical trajectory swarm in Fig. 7.5.3. Consider principle action.

$$S_p(\mathbf{0}, 0 : \mathbf{r}, t) = \int_0^t \mathbf{p} \cdot d\mathbf{r} - \int_0^t dt H = S_H(\mathbf{0} : \mathbf{r}) - Ht$$

Here, energy $H=E$ is assumed constant. If momentum is also constant then S_p reduces to

$$S_p(\mathbf{0}, 0 : \mathbf{r}, t) = \mathbf{p} \cdot \mathbf{r} - Ht = \hbar(\mathbf{k} \cdot \mathbf{r} - \omega t),$$

which is the plane-wave quantum phase times Planck's angular constant $\hbar=h/2\pi$. It is the time dependent principle action contours which actually move at a speed equal to the *quantum phase velocity*

$$\mathbf{V}_{phase} = \frac{d\mathbf{r}}{dt} = \frac{H}{\mathbf{p}} = \frac{\omega}{\mathbf{k}} \quad (7.5.20a)$$

This follows by setting $S_p=const.$ or

$$dS_p(\mathbf{0}, 0 : \mathbf{r}, t) = 0 = \mathbf{p} \cdot d\mathbf{r} - Hdt. \quad (7.5.20b)$$

This is quite the opposite of classical particle velocity which matches the *quantum group velocity*

$$\mathbf{V}_{group} = \frac{d\mathbf{r}}{dt} = \frac{\partial H}{\partial \mathbf{p}} = \frac{\partial \omega}{\partial \mathbf{k}} \quad (7.5.20c)$$

Consequently, when the particle velocity or momentum \mathbf{p} is highest the S_p phase velocity of the contours in Fig. 7.5.2 is slowest. High \mathbf{p} in Fig. 7.5.2 means high gradient $\nabla S_H = \mathbf{p}$ so the S_H contours are closer together. An S_p front moves from one $S_H = n2\pi$ contour to the next $S_H = (n+1)2\pi$ contour at frequency $\omega = H/\hbar$ so big \mathbf{p} means slow going. Note that the lower regions of each contour in Fig. 7.5.2 moves much slower than the upper regions; quite the opposite of the classical swarm circles in Fig. 7.5.3. Two "cat ears" move down rapidly until, like Carroll's Cheshire cat, nothing remains but its smile!

When classical momentum approaches zero, as at the top of Fig. 7.5.3b, the S_p wave phase speed diverges to infinity. This is when two "cat ears" are created which race out along the top of the classical envelope in Fig. 7.5.2b. Soon, they too slow down as the classical momentum again picks up.

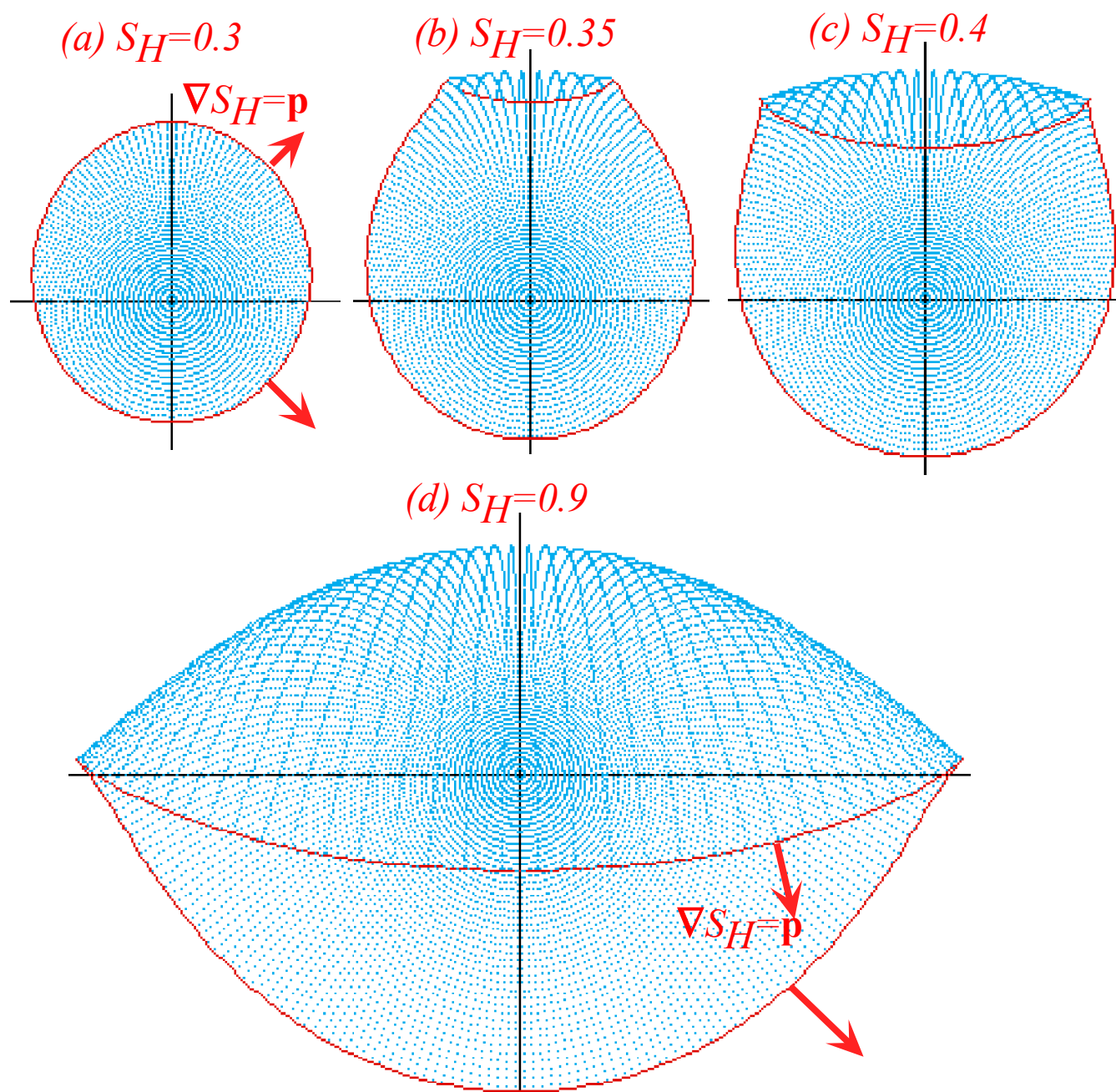


Fig. 7.5.2 Constant S_H contours for iso-energetic trajectory family are normal to trajectory paths.

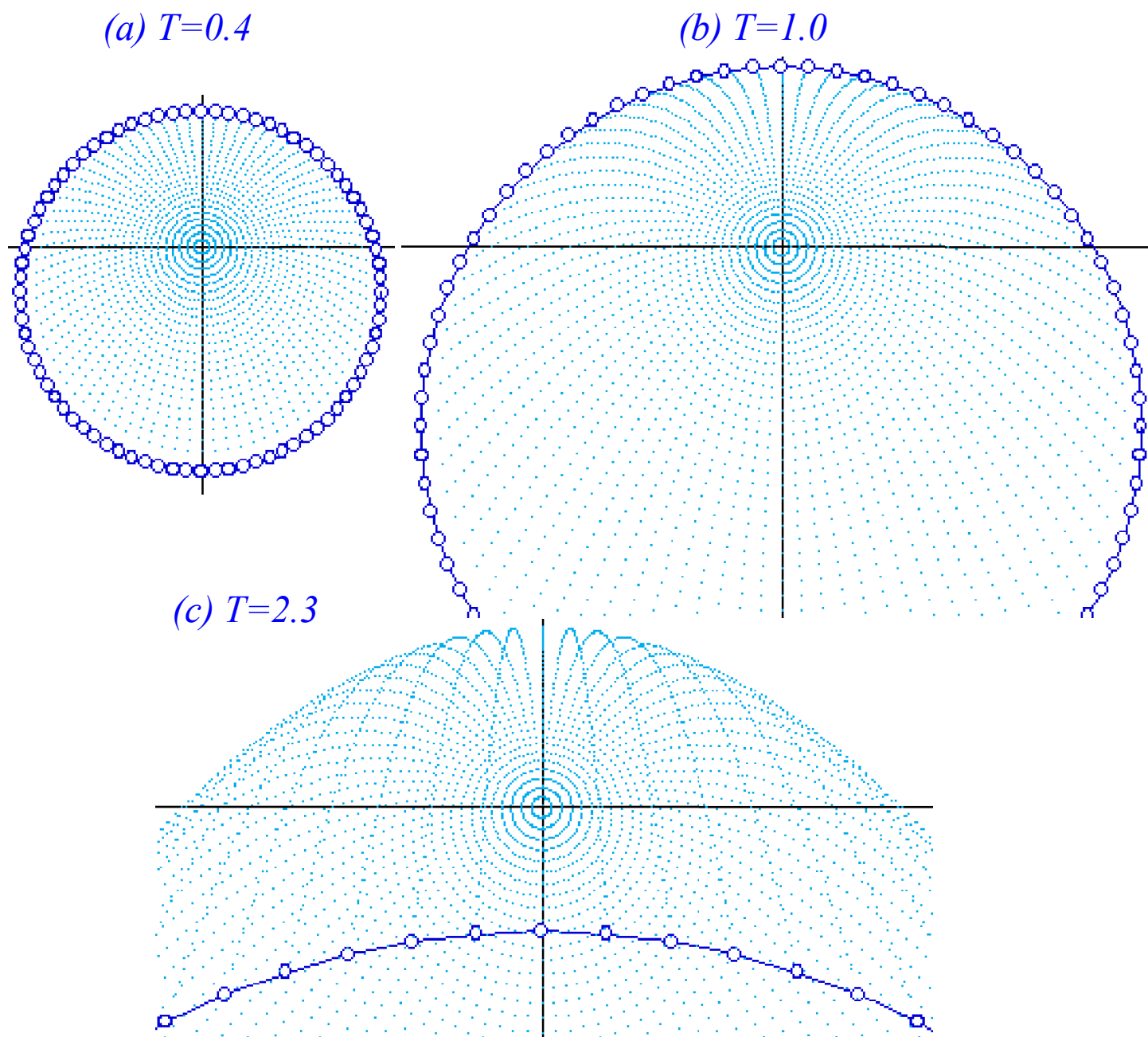


Fig. 7.5.3 Constant travel-time- T contours for iso-energetic trajectory family are circles.

Chapter 7.6 Time of Flight, Energy, and Action

Action formalism is generally reluctant to yield convenient analytic expressions since action, by its fundamental definitions (7.5.1) and (7.5.2), is an accumulation or integration. Also, action S_p or S_H has the units of Joule-seconds, that is, energy-time, so it is intertwined with two other extensive variables that are also based upon integration, work-energy $E=H$ and period or time of flight T .

Consider the time integrals of the form of the quadrature integrals first introduced in Units 2-3 (Equation (2.7.10b) or in (3.8.15)). Let a separable system have a conserved partial-Hamiltonian

$$\varepsilon = h(q,p) = p^2/2m + V(q) = \text{const.}, \quad (7.6.1a)$$

for each canonical variable q, q', \dots , so the total Hamiltonian and energy is a sum of the separate parts.

$$E = H(q, p, q', p', \dots) = h(q,p) + h'(q',p') + \dots = \varepsilon + \varepsilon' + \dots \quad (7.6.1b)$$

Then the time-of-flight from q_0 to q_1 is an integral

$$T = t_1 - t_0 = \int_{t_0}^{t_1} dt = \int_{q_0}^{q_1} dq \frac{dt}{dq} = \int_{q_0}^{q_1} \frac{dq}{\dot{q}} \quad (7.6.2)$$

where Hamilton's equation gives velocity \dot{q} in terms of momentum and conserved energy ε in (7.6.1).

$$\dot{q} = \frac{\partial H}{\partial p} = \frac{p}{m} = \frac{\sqrt{2m[\varepsilon - V(q)]}}{m} \quad (7.6.3)$$

The time-of-flight integral for coordinate q between q_0 and q_1 is as follows.

$$T = t_1 - t_0 = \int_{q_0}^{q_1} \frac{m dq}{p} = \int_{q_0}^{q_1} \frac{m dq}{\sqrt{2m[\varepsilon - V(q)]}} \quad (7.6.4)$$

The Hamilton characteristic or reduced action s_h has an integral related to the time integral.

$$s_h(q_0 : q_1) = \int_{q_0}^{q_1} p dq = \int_{q_0}^{q_1} dq \sqrt{2m[\varepsilon - V(q)]} \quad (7.6.5a)$$

There is one such integral for each separable coordinate q, q', \dots . The total action is a sum of such integrals.

$$S_H = s_h(q_0 : q_1) + s'_h(q'_0 : q'_1) + \dots = \int_{q_0}^{q_1} p dq + \int_{q'_0}^{q'_1} p' dq' + \dots = \sum_{\mu} \int_{q_0^{\mu}}^{q_1^{\mu}} p_{\mu} dq^{\mu} \quad (7.6.5b)$$

Each s_h is related by ε -derivative to its corresponding time of flight integral T, T', \dots for each q .

$$\frac{\partial S_H}{\partial \varepsilon} = \frac{ds_h}{dh} = T, \quad \frac{\partial S_H}{\partial \varepsilon'} = \frac{ds'_h}{dh'} = T', \quad \dots \quad \text{or:} \quad \frac{\partial S_H}{\partial \varepsilon_{\mu}} = \frac{ds_h^{\mu}}{dh_{\mu}} = T^{\mu} \quad (7.6.5c)$$

This is a general result based on a time-to-energy change of variable in each one-dimensional integral.

$$T = \int dt = \int \frac{dq}{\dot{q}} = \int \frac{dq}{\frac{dp}{dh}} = \int dq \frac{dp}{dh} = \frac{d}{dh} \int p dq = \frac{ds_h}{dh} \quad (7.6.6)$$

It is consistent with Poincare' relation $s_h = s_p + h t$ in (7.5.5h) since s_p is independent of energy $h=\varepsilon$.

(a) Quantum wave fronts vs. classical

Dirac and Feynman noted quantum wave function approximations using action as phase.

$$\psi(r, t) = \psi_0 e^{iS_p/\hbar} \quad (7.6.7)$$

If this approximation is substituted into the Schrodinger wave equation,

$$i\hbar \frac{\partial \psi(r, t)}{\partial t} = H\psi = -\frac{\hbar^2}{2m} \nabla^2 \psi + V(r)\psi \quad (7.6.8)$$

the result is an equation of the Riccati form.

$$\begin{aligned} -\psi \frac{\partial S}{\partial t} &= -\psi \frac{\hbar i}{2m} \nabla^2 S + \psi \left[\frac{1}{2m} \left(\frac{\partial S}{\partial \mathbf{r}} \right)^2 + V(r) \right] \\ \frac{\hbar i}{2m} \nabla^2 S &= \frac{\partial S}{\partial t} + \left[\frac{1}{2m} \left(\frac{\partial S}{\partial \mathbf{r}} \right)^2 + V(r) \right] = \frac{\partial S}{\partial t} + H \left(\frac{\partial S}{\partial \mathbf{r}}, \mathbf{r} \right) \end{aligned} \quad (7.6.9)$$

In the limit that the left hand double (Laplacian) derivative vanishes, the full quantum Schrodinger equation reduces to the classical HJ equation (7.5.5). This is sometimes called the *semi-classical limit*.

$$\hbar \left| \nabla^2 S \right| \ll \left(\frac{\partial S}{\partial \mathbf{r}} \right)^2, \text{ or: } \hbar \left| \frac{d^2 S}{dx^2} \right| = \hbar \left| \frac{dp_x}{dx} \right| \ll p_x^2, \text{ or: } \hbar \left| \frac{dp_x}{dx} \right| / |p_x| \ll |p_x| = \hbar |k_x| \quad (7.6.10a)$$

If this holds, then DeBroglie wavelength $\lambda_x/\hbar = 1/\hbar k_x = 1/p_x$ is small compared to its variation over one wavelength, or, equivalently wavevector k_x is large compared to relative rate of change of k_x .

$$\left| \frac{dk_x}{dx} \right| / |k_x| \ll |k_x|, \text{ or: } \left| \frac{d\lambda_x}{dx} \right| \ll 1 \quad (7.6.10b)$$

Since Planck's constant $\hbar = 1.054572E-34$ *Joule seconds* is so small, a classical particle with a modest momentum of *1 Joule second per meter* has an extraordinarily immodest wavevector: $k_x = p_x/\hbar = 9.4825 E 33$, that is, roughly $1/\lambda_x = 1.50919 E33$ or *1,509,190,000,000,000,000,000,000,000,000 wavelengths per meter*. Usually, a potential is not strong enough to make momentum vary appreciably over the 10^{-32} meters occupied by one such wave. The one exception is where momentum goes to zero and the wavelength blows up as it does on top of the envelope in Fig. 7.5.2. At such singularities the HJ-equations will part company with Schrodinger. Such points are the *classical turning points*.

(b) Huygen's principle: "Proof" of classical axioms

Enveloping curves generated by contact transformations are closely related to *Huygen's principle* of wave optics which applies to quantum waves of matter, as well. Consider a hypothetical action function $S_H(\mathbf{r}_0 : \mathbf{r})$ which might generate the curves $S_H(\mathbf{r}_0 : \mathbf{r}) = 10, 20$, and 30 as sketched in Fig. 7.6.1.

Now imagine the same generator acts starting from two points \mathbf{r}_{10} and \mathbf{r}'_{10} on the $S_H(\mathbf{r}_0 : \mathbf{r}) = 10$ wave front thereby generating two sets of intermediate wave fronts: $S_H(\mathbf{r}_{10} : \mathbf{r}) = 10$ and $S_H(\mathbf{r}'_{10} : \mathbf{r}) = 10$ around each of these two points. All points on these curves represent a total accumulation of *20 J's* of action since leaving \mathbf{r}_0 , but only for select points like \mathbf{r}_{20} and \mathbf{r}'_{20} is *20 J* the *least* action.

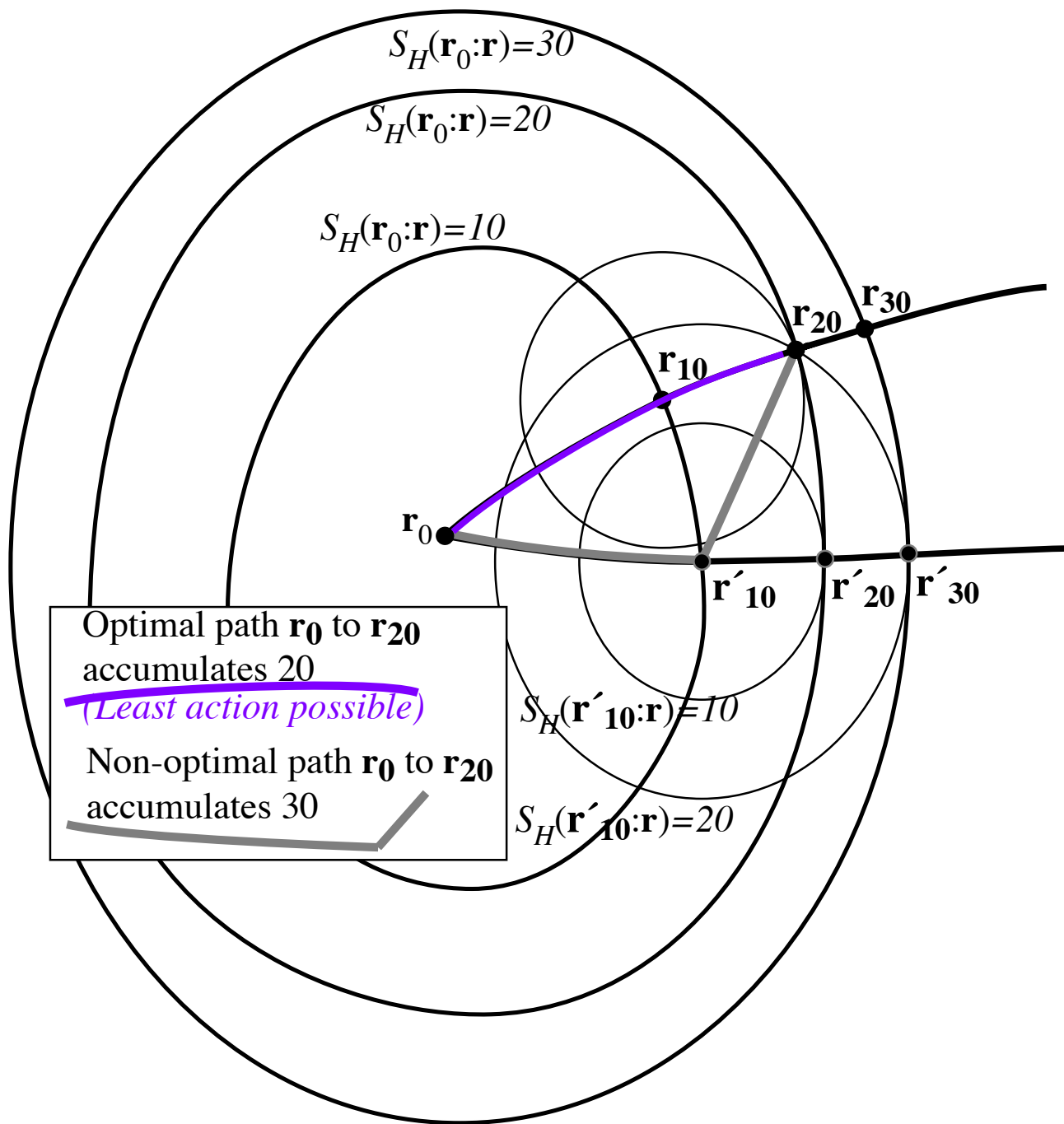


Fig. 7.6.1 Comparison of paths and wave fronts for discussion of Huygen's principle.

These special points $r=r_{20}$ and $r=r'_{20}$ of least action are just the contacting ones that lie on the envelope curve $S_H(r_0:r)=20$. They also lie on optimal (least action) trajectory paths from r_0 which have never failed to follow the undeviating "straight-and-narrow" paths determined by Lagrange equations. What makes these paths appear to follow the classical Lagrange equations? Why do they appear to optimize their action so faithfully? Huygens knew the answer in the 1600's, at least for rays of light. The key word here is "appear" since neither light waves nor matter waves originally have any intention of following a straight and narrow path!

Quite the contrary, every point on a Huygen's wave front broadcasts a continuum of deviant wave fronts in the form of the intermediate "wavelet" ovals such as $S_H(\mathbf{r}_{10} : \mathbf{r}) = I_0$ and $S_H(\mathbf{r}'_{10} : \mathbf{r}) = I_0$ in Fig. 7.6.1. But, for each of these non-optimal deviant "rascals" there are thousands more neighboring "rascals" whose actions differ enough that most paths end up canceling each other by destructive interference of the varying phases due to deviant actions. There is no honor amongst thieves!

Only for those optimal paths of stationary action (and therefore, stationary phase) do the phases add constructively, and it is only for these that quantum wave intensity or classical presence appears to exist most of the time in a classical world of enormous action. All paths are possible to varying degrees and exist in some sense, but only the optimal ones make their presence known and generally do so while obeying quite precisely the classical equations of motion.

In a sense, this constitutes an evolutionary proof of Newton's "laws" or at least justification of Newton's axioms in the case of high action or the classical limit. The classical world appears to be a result of a continual process of natural selection!

However, the situation is different for systems with discrete or limited number of paths as in the case of low action or when wavelength is comparable to the size of a system. Then the classical myth is likely to disintegrate like Dracula out of his coffin at dawn! Now matter how dearly we believe in our precisely machined gears and fine particles there comes a time and place where the classical equations part company with new reality, that is, with increasingly clever and precise experimental evidence.

Nevertheless, the classical apparatus is far too well developed to die forever, and it rises to assist the newly appointed quantum paradigm in what is called semi-classical approximation theory. The role of generating action functions $S_p(\mathbf{r}_0, t_0 : \mathbf{r}, t)$ and $S_H(\mathbf{r}_0 : \mathbf{r})$ is taken over in quantum theory by amplitudes, wavefunctions, or matrix elements such as the amplitude $\langle \mathbf{r}, t | \mathbf{r}_0, t_0 \rangle$ of time-evolution and or the transition-overlap amplitude $\langle \mathbf{r} | \mathbf{r}_0 \rangle$. Here, $|\langle \mathbf{B} | \mathbf{A} \rangle|^2$ is the probability for a state-**A** to become state-**B** if forced to make a choice. Bracket $\langle \mathbf{B} | \mathbf{A} \rangle$ is called a *probability amplitude*; past-to-future is read right-to-left like Hebrew. Probability amplitudes may be approximated by semi-classical relations similar to (7.6.7).

$$\langle \mathbf{r}_1, t_1 | \mathbf{r}_0, t_0 \rangle = e^{iS_p(\mathbf{r}_0, t_0 : \mathbf{r}_1, t_1)/\hbar} \quad (7.6.11a) \quad \langle \mathbf{r}_1 | \mathbf{r}_0 \rangle = e^{iS_H(\mathbf{r}_0 : \mathbf{r}_1)/\hbar} \quad (7.6.11b)$$

Restating Huygen's principle with semiclassical amplitudes gives a *completeness* or *closure* relation.

$$\sum_{\mathbf{r}'} \langle \mathbf{r}_1 | \mathbf{r}' \rangle \langle \mathbf{r}' | \mathbf{r}_0 \rangle \cong \sum_{\mathbf{r}'} e^{i(S_H(\mathbf{r}_0 : \mathbf{r}') + S_H(\mathbf{r}' : \mathbf{r}_1))/\hbar} = e^{iS_H(\mathbf{r}_0 : \mathbf{r}_1)/\hbar} = \langle \mathbf{r}_1 | \mathbf{r}_0 \rangle \quad (7.6.12)$$

Intermediate \mathbf{r}' -path sums, as in Fig. 7.6.1, cancel by phase variation except on the optimal stationary-action path $\mathbf{r}_1 \leftarrow \mathbf{r}_0$. The sum over phase factors from \mathbf{r}' -paths is well approximated by the amplitude for the stationary optimal path. Methods for summing over all paths (including deviant ones) are called Feynman path integration techniques. Often, this extra effort is not needed.

Chapter 7.7 Action-Angle Variables : Semi-classical quantization

(a) 1-Dimensional vibration and rotation

For a vibrating coordinate q it is convenient to define a *single-period-action* Σ_H as follows.

$$\Sigma_H(q_0) \equiv S_H(q_0 : q_0) = \oint_{q_0 \rightarrow q_0} p dq \quad (7.7.1)$$

This makes sense if the q -coordinate lies on a closed loop in its phase space as indicated in Fig. 7.7.1a. This example, a pendulum phase plot, has loops for energies below the separatrix where it can vibrate or swing starting at some amplitude $q_0 = \theta_0$ and eventually returning to that amplitude q_0 after one full period $T = \tau$. Above the separatrix, the pendulum angle is no longer bound. Then the pendulum ceases to be a *vibrator* and becomes a *rotator* whose angle increases more or less steadily: $\theta_0 \rightarrow \theta_0 + 2\pi \rightarrow \theta_0 + 4\pi$ and so on as in Fig. 7.7.1b. In this case we re-define the single-period action.

$$\Sigma_H(p_0) \equiv S_H(q_0 : q_0 + 2\pi) = \int_{q_0}^{q_0 + 2\pi} p dq \quad (7.7.2)$$

In either case, the single-period action is a phase space area for one period as sketched in Fig. 7.7.1. The coordinate or momentum dependence of these single-period actions is actually somewhat redundant; Σ_H depends on *choice* of path and not on any point on the path. Each Σ_H path is a phase-space topography line of a particular energy or Hamiltonian value $H = E$, and that is the primary dependency of the Σ_H actions.

According to (7.6.5c) the energy or Hamiltonian dependence is related to the oscillation period.

$$\frac{d\Sigma_H}{dH} = \frac{d\Sigma_H}{dE} = T(\text{single-period}) = \tau \quad (7.7.3)$$

The inverse of this is a frequency of vibration (or rotation).

$$\frac{dH}{d\Sigma_H} = \frac{dE}{d\Sigma_H} = \frac{1}{T(\text{single-period})} = \nu = \frac{\omega}{2\pi} \quad (7.7.4)$$

It is conventional to write this in the form of one of Hamilton's equations

$$\frac{dH}{d\Sigma_H} = \frac{\omega}{2\pi} \quad \text{becomes:} \quad \frac{dH}{dJ} = \omega \equiv \dot{\theta} \quad (7.7.5a)$$

where the *action-angular-momentum* J is defined as follows.

$$J = \frac{\Sigma_H}{2\pi} \equiv \begin{cases} \frac{1}{2\pi} \oint_{q_0 \rightarrow q_0} p dq & \text{(for vibrator)} \\ \frac{1}{2\pi} \int_{q_0}^{q_0 + 2\pi} p dq & \text{(for rotator)} \end{cases} \quad (7.7.5b)$$

Action-momentum J is conjugate to an *action-angle-variable* or simply *action-angle* defined as follows.

$$\theta = \omega t + \theta_0 \quad (7.7.6)$$

The other Hamiltonian equation is simple; H has no θ -coordinate dependence and so J is conserved.

$$\frac{dH}{d\theta} = 0 \equiv J \quad \text{or:} \quad J = \text{const.} \quad (7.7.7)$$

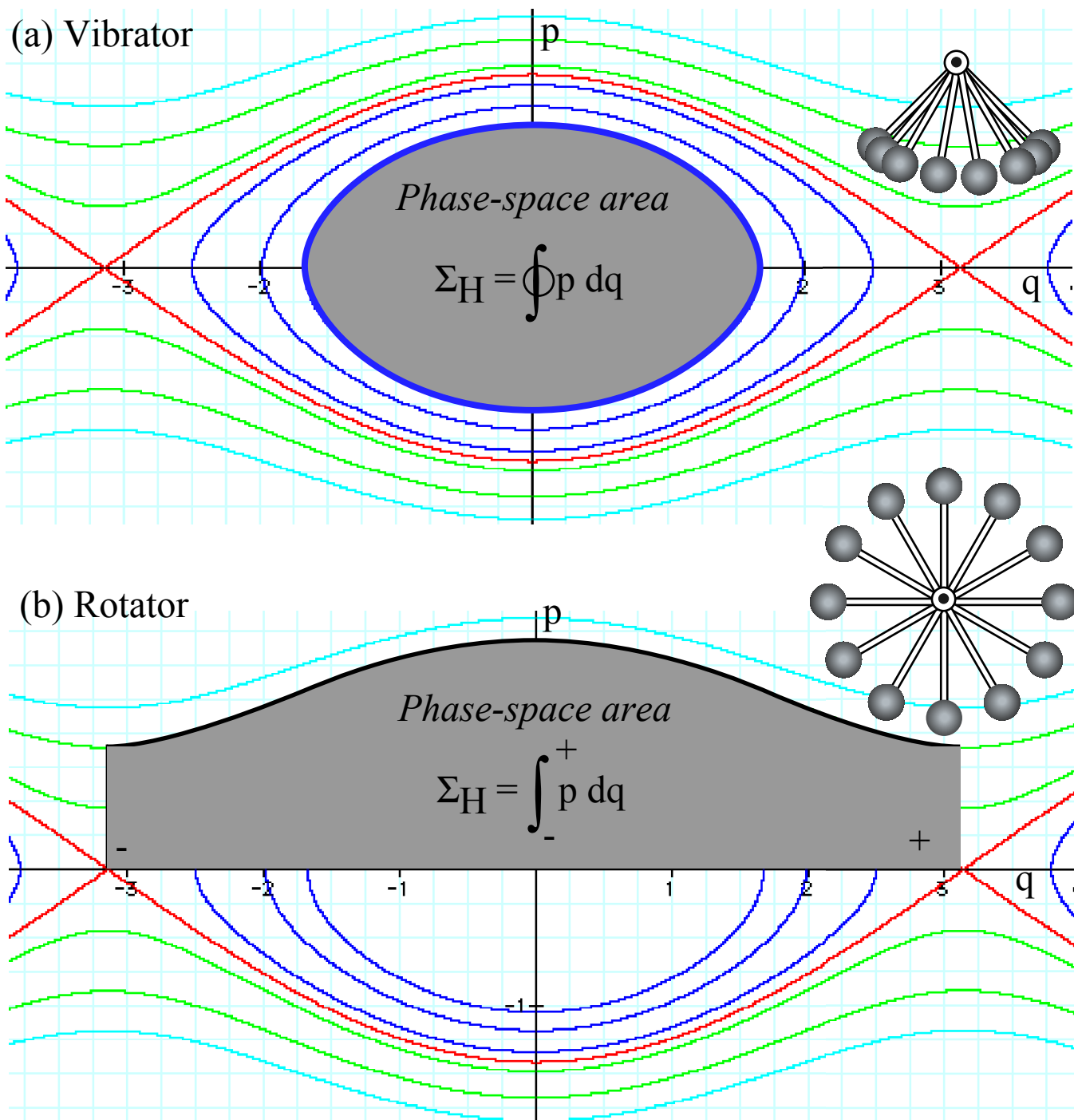


Fig. 7.7.1 Comparison of phase space area or action momentum for (a) Vibrator and (b) Rotator.

The simplest action Hamiltonian is the *harmonic oscillator* which is *linear* in its action momentum.

$$H_{\text{harmonic}} = \omega J \tag{7.7.8}$$

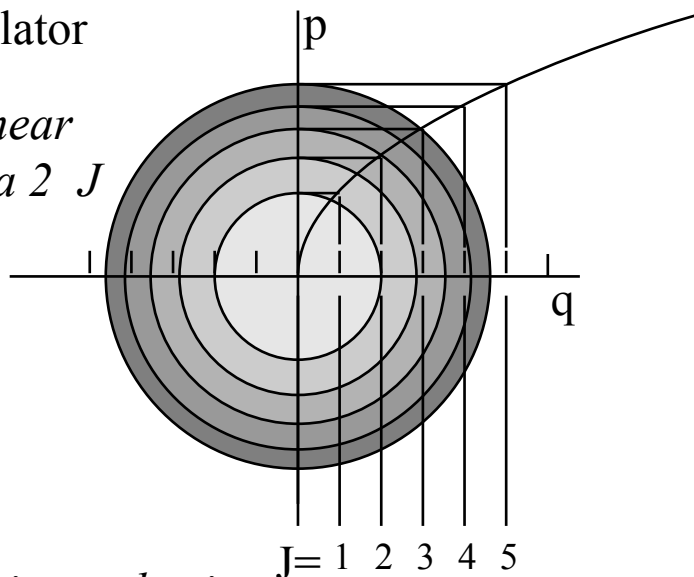
The *free-rotor* is, perhaps, the next simplest action Hamiltonian. It is *quadratic* in action momentum.

$$H_{\text{free}} = B J^2 \tag{7.7.9}$$

These cases are sketched in part (a) and (b) of Fig. 7.7.2. In either case, the kinetic energy $p^2/2I$ is quadratic in the original momentum variable p . Harmonic oscillator energy is quadratic in coordinate q , as well, for harmonic potential $1/2kq^2$. The free rotor has no potential so $J=p$.

(a) Harmonic oscillator

Energy $H = \omega J$ is linear
in phase-space area $2 J$



(b) Free rotor

Energy $H = BJ^2$ is quadratic
in phase-space area $2 J$

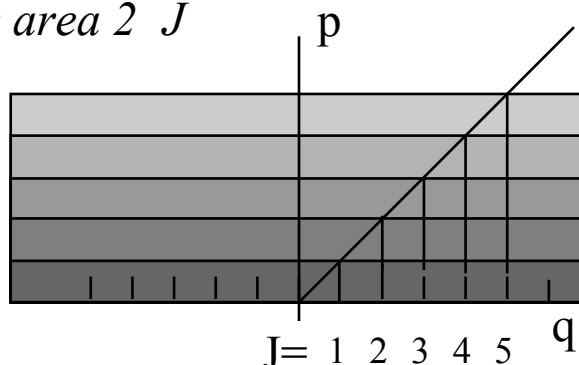


Fig. 7.7.2 Comparison of phase space area or action for (a) Harmonic oscillator and (b) Free rotor.

Phase space area $\Sigma_H = 2\pi J$ is a key quantity in quantum theory since each state is allowed a patch of phase space area that is an integer multiple of Planck's constant $\hbar = 6.62607E-34$ Joule seconds. This is called a *Bohr quantization* relation. Using Planck's angular constant $\hbar = h/2\pi = 1.054572E-34$ we have

$$J = \text{Area in } (p,q) / 2\pi = \hbar \nu. \tag{7.7.10a}$$

The integer ν ($\nu = 0, 1, 2, \dots$) is a *quantum number*. Bohr quantization is a result of requiring the quantum amplitude (7.6.11b) to be unity for each closed loop or full period, as follows.

$$I = \langle \mathbf{r}_0 | \mathbf{r}_0 \rangle = e^{iS_H(\mathbf{r}_0; \mathbf{r}_0) / \hbar} = e^{i\Sigma_H / \hbar}, \text{ or: } \Sigma_H = 2\pi \hbar \nu = 2\pi J \tag{7.7.10b}$$

(b) Multi-dimensional action angle analysis

Once again we suppose that an N -dimensional Hamiltonian is separable, as in the example of (7.5.8) in Sec. 7.5.(c), into N independent 1-dimensional parts. Let the H-J partial differential equation

$$\begin{aligned} \text{const.} = E = H(p_1, p_2, \dots, q^1, q^2, \dots) &= H\left(\frac{\partial S_H}{\partial q^1}, \frac{\partial S_H}{\partial q^2}, \dots, q^1, q^2, \dots\right) \\ &= \varepsilon_1 + \varepsilon_2 + \dots = h_1\left(\frac{ds_{h1}}{dq^1}, q^1\right) + h_2\left(\frac{ds_{h2}}{dq^2}, q^2\right) + \dots \end{aligned} \quad (7.7.11a)$$

separate into N ordinary differential equations

$$\text{const.} = \varepsilon_1 = h_1\left(\frac{ds_{h1}}{dq^1}, q^1\right), \quad \text{const.} = \varepsilon_2 = h_2\left(\frac{ds_{h2}}{dq^2}, q^2\right), \quad \dots \quad (7.7.11b)$$

with each contributing a term to the total characteristic action.

$$S_H(q_A^1, q_A^2, \dots, q_B^1, q_B^2, \dots) = \int_{q_A^1}^{q_B^1} p_\lambda dq^\lambda = s_{h1}(q_A^1 : q_B^1) + s_{h2}(q_A^2 : q_B^2) + \dots \quad (7.7.11c)$$

If each part was a bound system, that is a vibrator or rotator like those discussed in Sec. 5.7(a), then it has separate single-period-action-angles (J_m, θ^m) with the following action momentum J_m .

$$J_1 = \frac{\Sigma_{h1}}{2\pi} = \frac{1}{2\pi} \oint p_1 dq^1, \quad J_2 = \frac{\Sigma_{h2}}{2\pi} = \frac{1}{2\pi} \oint p_2 dq^2, \quad \dots \quad (7.7.12a)$$

The Hamilton's equations for each part are like those of (7.7.5) and (7.7.7).

$$\begin{aligned} \frac{\partial H}{\partial J_1} = \theta^1 = \omega_1, \quad \frac{\partial H}{\partial J_2} = \theta^2 = \omega_2, \quad \dots \\ -\frac{\partial H}{\partial \theta^1} = 0 = J_1, \quad -\frac{\partial H}{\partial \theta^2} = 0 = J_2, \quad \dots \end{aligned} \quad (7.7.12b)$$

Because $H = H(J_1, J_2, \dots)$ is a function only of J 's and not angles θ^m , both enjoy simple time behavior.

$$\begin{aligned} \theta^1(t) = \omega_1 t + \theta^1(0), \quad \theta^2(t) = \omega_2 t + \theta^2(0), \quad \dots \\ J_1 = \text{const.} = \hbar n_1, \quad J_2 = \text{const.} = \hbar n_2, \quad \dots \end{aligned} \quad (7.7.12c)$$

In the last line we have taken the liberty of imposing semi-classical Bohr quantization conditions (7.7.10) on the action momentum values. This would give the approximate quantum energy levels of this system when substituted into the Hamiltonian function of action momentum.

$$E_{n_1 n_2 \dots} = H(\hbar n_1, \hbar n_2, \dots) \quad (7.7.13)$$

Given the intractable algebra of action calculus, we surmise that finding all the preceding quantities is, at best, a tall order, and at worst not possible. Analytic action angle solutions are possible only for a fairly select class of cases, most notably the Coulomb and harmonic oscillator potentials and field-free rigid symmetric rotors. Fortunately, numerical approximation methods again may come to the rescue as they did for the parabolic trajectory problem treated earlier in Sec. 7.6.

(c) Action-color and Davis-Heller quantization

The method of characteristics which found the $S_H(\mathbf{r}_0 : \mathbf{r})$ curves in the trajectory example of Fig. 7.5.2 may be extended to find Σ_H and J values, as well. But, there are differences between open trajectory systems and closed systems of bound vibrators or rotators. Arbitrary energy and action are valid classical and quantum-approximate values in the case of unbounded trajectories, but only certain *quantizing* values of energy and action make sense for bound or closed systems. Some scheme is needed to solve for the Bohr quantization conditions (7.7.10), (7.7.12c) or something equivalent to them.

A colorful way to display action and its Bohr quantization is to numerically integrate Hamilton's equations and Lagrangian L and color the trajectory according to the current accumulated value of action

$$S_H(\mathbf{0} : \mathbf{r}) = S_p(\mathbf{0}, 0 : \mathbf{r}, t) + Ht = \int_0^t L dt + Ht .$$

The hue should represent the phase angle $S_H(\mathbf{0} : \mathbf{r})/\hbar \text{ modulo } 2\pi$ as, for example, $0=\text{red}$, $\pi/4=\text{orange}$, $\pi/2=\text{yellow}$, $3\pi/4=\text{green}$, $\pi=\text{cyan}$ (opposite of red), $5\pi/4=\text{indigo}$, $3\pi/2=\text{blue}$, $7\pi/4=\text{purple}$, and $2\pi=\text{red}$ (full color circle). Interpolating action on a palette of 32 colors is enough precision for low quanta.

The colored paths display a confused gray mess if phases fail to interfere constructively. But, for select quantizing values of energy, there appear striking patterns of colors when Bohr quantization makes phases interfere constructively. Patterns are outlines of quantum waves based on (7.6.11b).

$$\langle \mathbf{r}_1 | \mathbf{r}_0 \rangle = e^{iS_H(\mathbf{r}_0 : \mathbf{r}_1)/\hbar} \quad (7.7.14a)$$

This *color-quantization* technique was first done on a CRAY-*Dicomed* film system by Heller and Davis in 1983. Now it can be done on practically any personal computing system.

A quantizing example for a 2-dimensional oscillator using the *ColorU(2)* program is shown in Fig. 7.7.3. Viewing this in gray-scale is possible since only two hues actually survive: *red*, representing a phase of 0 , and *cyan*, representing a phase of π . The example is a standing wave mode in (x,y) -coordinate space, so the only possible wave amplitude is ± 1 , that is, complimentary hues *red* and *cyan* which appear as light and dark gray in a gray scale portrait. The remaining colors pile up on the nodal lines where the waves' many action phases are destructively interfering amplitude to near-zero values.

An addition to the color quantization technique also displays the principle (time-dependent) action $S_p(\mathbf{0}, 0 : \mathbf{r}, t)$ and the time-dependent wave from (7.6.11a)

$$\langle \mathbf{r}_1, t_1 | \mathbf{r}_0, t_0 \rangle = e^{iS_p(\mathbf{r}_0, t_0 : \mathbf{r}_1, t_1)/\hbar} = e^{iS_H(\mathbf{r}_0 : \mathbf{r}_1)/\hbar - i\omega \cdot T} \quad (7.7.15a)$$

where

$$T = t_1 - t_0, \quad \text{and: } H = \hbar\omega \quad (7.7.15b)$$

This gives an animated display of phase velocity (7.5.20a). It is done by rotating the color spectrum of the computer in accordance with the time-dependent phase angle Ht in (7.7.15). By making two of the entries in the phase-color palette to be black-and-white it is possible to display a wave front line which will march in step with the other hues in the palette and create the on-screen illusion of moving wave fronts.

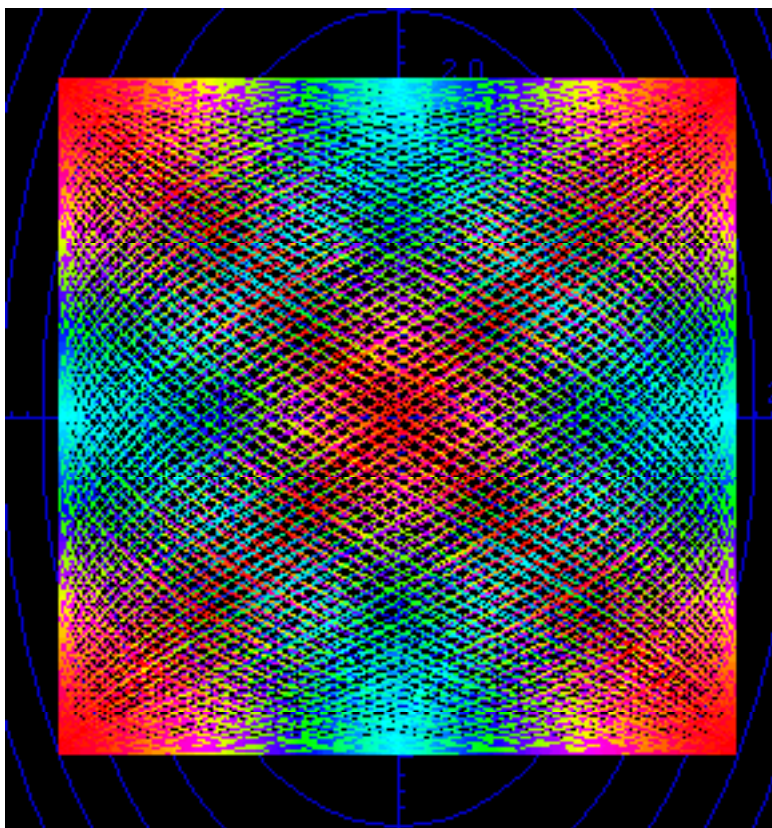


Fig. 7.7.3 Phase-color 2-dimensional harmonic oscillator paths showing $(2,2)$ quantum wave function.

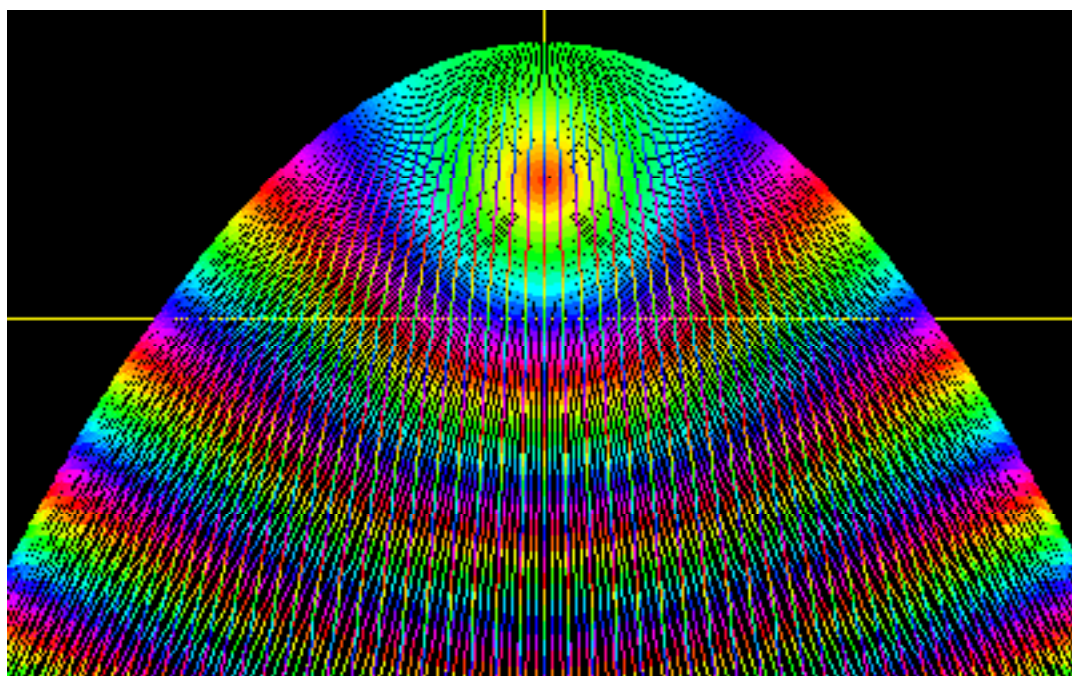


Fig. 7.7.4 Phase-color trajectory paths showing quantum wave fronts.

An example of action-colored trajectories in Fig. 7.7.4 is to be compared with Fig. 7.5.2.

(d) A "clockwork universe"

A dream of the 1800's classical mechanics was a "clockwork universe." Hamilton, Jacobi and other contemporaries almost achieved this dream with their action-angle formalism. We say, "almost," because it works only for *separable* systems. The dream fails for many mechanical systems which are non-separable. (Some might say, this includes virtually *all* real systems.) Non-separable systems (including the ancient *trebuchet*) generally exhibit *stochastic* or "chaotic" behavior.

Nevertheless, let us suppose we have a separable system that conforms to the 1800's dream and reduces to set of N action-angle equations like (7.7.12a-b). In other words, we are able to find a $2N$ -dimensional phase space $((J_1, \theta_1), (J_2, \theta_2), \dots, (J_N, \theta_N))$ in which all the momenta are constants $J_m = \text{const.}$, and all the coordinates follow straight-line time trajectories of constant angular velocity ω_m .

$$\theta_m(t) = \omega_m t + \theta_m(0) \quad (7.7.16)$$

This is a *Bunyanesque* coordinate-momentum transformation! (Recall the mythical Paul Bunyan ox who was strong enough to straighten the crooked roads in Minnesota.) The action angles are a generalization of normal mode transformation of Section 4.3 that gives normal mode phase pairs (p_m, q^m) . Each phasor moves like a clock at a normal mode eigenfrequency ω_m . Together the clocks orchestrate all possible oscillator orbits. Together, N straight lines map onto all possible orbit curves.

Perhaps, the great success of normal mode analyses set the stage for the Hamilton-Jacobi dream of a clockwork universe. Little did the dreamers know that their dream was to be realized in the following century by a new quantum theory. As shown in Section 2.5, a quantum Schrodinger equation (2.5.1) is equivalent to a classical harmonic oscillator Hamiltonian (2.5.3). Schrodinger eigenstates correspond to normal modes of an analogous oscillator. To each mode- m or eigenstate $|\epsilon_m\rangle$ belongs a harmonic phasor clock Ψ_m of a complex exponential or probability amplitude.

$$\Psi_m(t) = |\Psi_m(0)| e^{-i\omega_m t} = x_m + i p_m \quad (7.7.17a)$$

Each eigenstate represents one "note" in a quantum orchestra that "plays" all possible states; the probability for the m -th "note" or m -th energy eigenstate is $\Psi_m^* \Psi_m$ which is proportional to the m -phasor area.

$$m\text{-phasor area} = \pi \Psi_m^* \Psi_m = \pi(x_m^2 + p_m^2) \quad (7.5.17b)$$

It is likely that the classicists might regard the quantum realization of their clockwork dream to be something of a Pyrrhic victory. They might be dismayed by the sheer number of oscillators needed to accurately describe most systems. (Even the 2-dimensional oscillator problem such as in Fig. 7.7.3 with an action of 1 Joule second would involve roughly 10^{33} clocks!) The classicist might also be dismayed by the seeming lack of precision in the probabilistic nature of the quantum amplitudes (7.7.17) where the phase space area or action momentum $2\pi J$ for the classical analog oscillator is just its probability. (Recall Einstein's plaintive quote, "God does not play dice with the universe!")

Many current physicists are classicists at heart. Virtually all physicists can at least appreciate the motivation for seeking a clockwork universe. However, such old classical myth suffers irreparably in the face of overwhelming evidence of just how "dicey" fundamental quantum processes really are.

(e) Non-linear modes: Action Fourier analysis

Despite the strong analogy between action-angle formalism and normal mode analysis, there needs to be emphasized some important differences. Normal mode analysis of Section 2.3 as well as the quantum analogy of Section 2.6 require *harmonic* oscillators which have *linear* (Hooke's law) spring force couplings. The word *harmonic* means all frequencies are independent of oscillator amplitude, and *linear* means if $q^m(t)$ and $q^{m'}(t)$ are each valid solution functions of the oscillator equations, then any multiples $2q^m(t)$, $3q^{m'}(t)$, etc., or any linear combination $2q^m(t)+3q^{m'}(t)$ of the solutions are valid, too. Together, harmonic and linear force equations guarantee that each normal mode of the system is perfectly *sinusoidal*, that is, a simple sine ($\sin \omega_m t$), cosine ($\cos \omega_m t$), or exponential ($e^{\pm i\omega_m t}$) of a single mode frequency ω_m . The general coordinate is a real linear combination of such modes.

$$x(t) = \sum_m (a_m^* e^{i\omega_m t} + a_m e^{-i\omega_m t}) \tag{7.7.18}$$

A force linear in coordinate x , such as $F_{linear}(x) = kx$, acting on sinusoidally varying coordinates preserves frequency spectrum $\{\omega_1, \omega_2, \dots, \omega_N\}$ by producing only those components already present.

$$F_{linear}(x(t)) = \sum_m (ka_m^* e^{i\omega_m t} + ka_m e^{-i\omega_m t}) \tag{7.7.19}$$

In contrast, a *nonlinear* force such as $F_{nonlinear}(x) = kx^2$ gives new frequency components.

$$\begin{aligned} F_{nonlinear}(x(t)) &= k(x(t))^2 \\ &= k \sum_m \sum_{m'} \left(a_m^* e^{i\omega_m t} + a_m e^{-i\omega_m t} \right) \left(a_{m'}^* e^{i\omega_{m'} t} + a_{m'} e^{-i\omega_{m'} t} \right) \\ &= k \sum_m \sum_{m'} \left(a_m^2 e^{i2\omega_m t} + a_m^* a_{m'}^* e^{i(\omega_m + \omega_{m'}) t} + a_m^* a_{m'} e^{i(\omega_m - \omega_{m'}) t} + \dots \right) \end{aligned}$$

The new components $\{2\omega_1, 2\omega_2, \dots, 2\omega_N\}$ are called *harmonic overtones* or *combination tones* $\{\omega_1 + \omega_2, \omega_2 + \omega_3, \dots\}$ or *difference tones* $\{\omega_1 - \omega_2, \omega_2 - \omega_3, \dots\}$. Each term drives the coordinates at these frequencies which then cause the non-linear force to make more harmonics of harmonics or combinations, and so on. Nonlinear forces with fractional power laws such as $F_{nonlinear}(x) = jx^{1/2}$ may also generate *subharmonic tones* $\{1/2\omega_1, 1/3\omega_1, \dots, 2\omega_N\}$. Such a cacophony of frequencies often leads to chaotic motion.

The action-angle formalism is a generalization of the normal mode analysis to separable systems that are *non-linear* and *anharmonic*. An example of a nonlinear system is a pendulum, whose phase space is shown in Fig. 7.7.1 and Fig. 7.7.5. (Recall also Fig. 1.15.1.) A pendulum has a non-linear $mg\sin\phi$ gravitational force law that is only approximately linear for small angle $\phi \ll 1$.

As shown in Fig. 7.7.5b, the non-linearity makes pendulum frequency anharmonic, that is, amplitude-dependent. As the amplitude approaches the separatrix ($\phi(0) \rightarrow \pm\pi$) the pendulum period gets longer ($\tau \rightarrow \infty$), frequency slows ($\omega \rightarrow 0$), and its trajectory becomes less sinusoidal. The result is a Fourier series of ω -overtones $\{\omega, 2\omega, 3\omega, 4\omega, \dots\}$, that is, $\phi(t)$ is a real *asinusoidal* function of period $\tau = 2\pi/\omega$.

$$\phi(t) = f_1^* e^{i\omega t} + f_1 e^{-i\omega t} + f_2^* e^{i2\omega t} + f_2 e^{-i2\omega t} + f_3^* e^{i3\omega t} + f_3 e^{-i3\omega t} + \dots \tag{7.7.20a}$$

The Fourier coefficients f_k are expressed in terms of an inversion integral (Recall (4.6.5b).)

$$\phi(t) = \sum_{k=-\infty}^{\infty} f_k e^{-ik\omega t} \quad \text{where: } f_k = \frac{1}{\tau} \int_{-\tau/2}^{\tau/2} dt \phi(t) e^{ik\omega t} \quad (\tau = 2\pi / \omega) \tag{7.7.20b}$$

The spectrum shown in Fig. 7.7.5d has a 3rd-overtone (three times fundamental) amplitude $f_3 \sim (1/3)f_1$, not unlike the square wave spectrum discussed in Unit 4. (Recall Fig. 4.6.2 and Fig. 4.6.11.) This is consistent with the non-sinusoidal time plot in Fig. 7.7.5d which is like a rounded square wave. Rounding reduces the f_5 or f_7 components to values well below what they are for a truly square wave.

Action angle coordinates are defined as in (7.7.12) by $\theta = \omega t$ and $d\theta = \omega dt$ to redo (7.7.20b).

$$\phi(t) = \sum_{k=-\infty}^{\infty} f_k e^{-ik\theta} \quad \text{where: } f_k = \frac{1}{2\pi} \int_0^{2\pi} d\theta \phi(\theta/\omega) e^{ik\theta} = f_{-k}^* \quad (7.7.20c)$$

The resulting action-angle Hamilton equation for coordinate derivatives follows.

$$\frac{\partial H}{\partial J} = \dot{\phi}(t) = \frac{d\phi}{dt} = -i\omega \sum_{k=-\infty}^{\infty} k f_k e^{-ik\theta} \quad (7.7.20d)$$

Pendulum momentum is asinusoidal, too, with its Fourier coefficients p_k obtained similarly to above.

$$p_\phi(t) = p_1^* e^{i\omega t} + p_1 e^{-i\omega t} + p_2^* e^{i2\omega t} + p_2 e^{-i2\omega t} + p_3^* e^{i3\omega t} + p_3 e^{-i3\omega t} + \dots$$

$$p_\phi(t) = \sum_{k=-\infty}^{\infty} p_k e^{-ik\theta} \quad \text{where: } p_k = \frac{1}{2\pi} \int_0^{2\pi} d\theta p_\phi(\theta/\omega) e^{ik\theta} = p_{-k}^* \quad (7.7.20e)$$

This leads to a Fourier formula for the single-period action momentum J .

$$J = \frac{1}{2\pi} \int_0^{2\pi} p_\phi d\phi = \frac{1}{2\pi} \int_0^\tau p_\phi \frac{d\phi}{dt} dt$$

$$= \frac{1}{2\pi} \int_0^\tau \left(\sum_{k'=-\infty}^{\infty} p_{k'} e^{-ik'\theta} \right) \left(-i\omega \sum_{k=-\infty}^{\infty} k f_k e^{-ik\theta} \right) dt \quad (7.7.20f)$$

$$= -i \sum_{k=-\infty}^{\infty} k p_{k'} f_k \frac{1}{2\pi} \int_0^\tau e^{-i(k'+k)\theta} d\theta = -i \sum_{k=-\infty}^{\infty} k p_{-k} f_k$$

$$= -i \sum_{k=-\infty}^{\infty} k p_k^* f_k$$

Fourier coefficients are time independent quantities by definition, that is, they are conserved constants of the motion. Therefore, it is reasonable to expect that the conserved action-momentum J to be expressed in terms of Fourier coefficients. If the Fourier coefficients can be derived numerically, then so can the J values. Always test such calculations by reproducing the classical motion using the derived $f_k e^{-ik\theta}$.

Fourier theory applies also to multi-dimensional systems and is the basis of computer action angle quantization techniques developed by Ezra and others. However, this method runs into problems for cases in which the number of Fourier harmonics becomes large and unmanageable as happens in regions of the phase space where chaotic motion prevails.

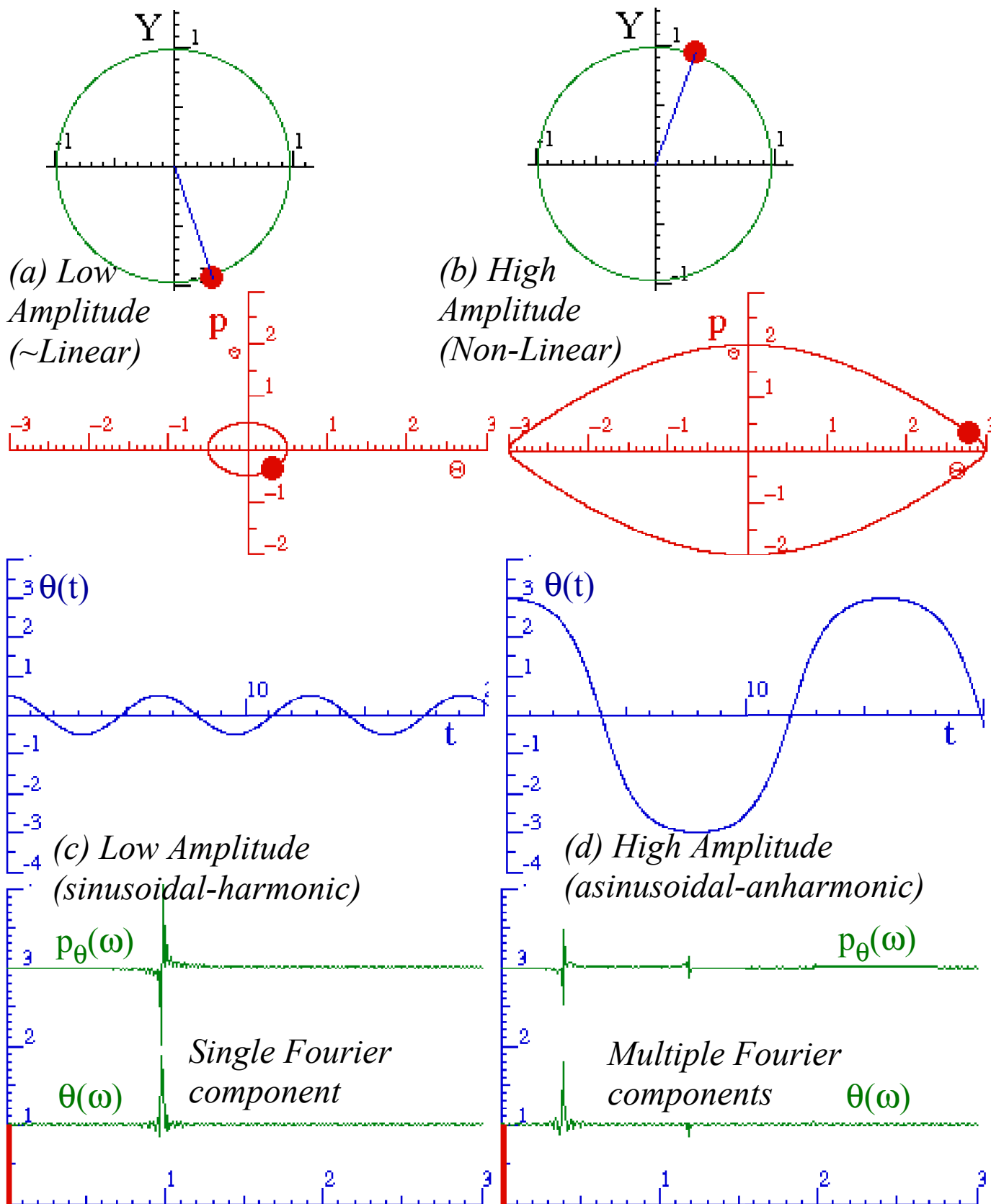


Fig. 7.7.5 Comparison of pendulum dynamics (a) Small amplitude. (b) Large amplitude.